PREDICTIONS OF SEISMIC MOTION AND CLOSE-IN EFFECTS

RULISON EVENT

ENVIRONMENTAL RESEARCH CORPORATION

AUGUST, 1969

2-4-5

NVO 1163-180

PREDICTIONS OF SEISMIC MOTION AND CLOSE-IN EFFECTS RULISON EVENT

COPY

by

B. G. Weetman

R. H. Berry
L. L. Davis
P. P. deCaprariis
W. W. Hays
R. A. Mueller
J. R. Murphy
D. L. Orphal
C. T. Spiker

Environmental Research Corporation
813 North Royal Street
Alexandria, Virginia

Prepared under
Contract No. AT(29-2)-1163
for the
Nevada Operations Office
U.S. Atomic Energy Commission

This page intentionally left blank

TABLE OF CONTENTS

LIST OF APPENDICES

LIST OF ILLUSTRATIONS

LIST OF ILLUSTRATIONS

(Continued)

LIST OF ILLUSTRATIONS

(Continued)

LIST OF TABLES

ABSTRACT

This report contains predictions of seismic motion and close-in effects for the Rulison event, development of prediction methods and pertinent geologic data. Some of the major features of the report are:

- Predictions of peak particle motion for selected locations
- Predictions of distances to peak particle motions of 0.1 g and 0.001 g (Accelerations)
- Predicted Pseudo-Relative Velocity (PSRV) Spectra at selected stations
- Geologic environment
- Development of seismic prediction method
- Predictions of cavity, cracking and gamma-radioactivity radii
- Predictions of chimney height and surface spalling

There is a discussion of each of the above with regard to procedure and results. Graphs and equations are provided.

This page intentionally left blank

Chapter 1
INTRODUCTION

The predictions herein are based on the predicted maximum yield, design yield, and other data summarized below.

Name of Event	Rulison
Hole Number	R-E
Depth of Burial	8,442.5 feet
Depth and Diameter of Casing	**8,453 feet x** 9.6 inches
Shot Medium	Shale and Sandstone

	Maximum Yield	Design Yield
Yields	60 kt	40 kt

Included in this report are predictions of close-in effects (cavity radius, chimney height, cracking radius, radius of gamma radioactivity), peak ground motions for selected locations and distances to 0.1 g and 0.001 g accelerations. In addition, Pseudo-Relative Velocity (PSRV) versus period predictions are made for selected stations. Chapter 2 summarizes all predicted quantities. The geology in the vicinity of the Rulison drill hole is discussed in Chapter 3. Chapter 4 discusses the predictions of the close-in effects associated with an underground nuclear detonation. The methods used to predict ground motions for the Rulison event are described in Chapter 5. Chapter 6 describes the effects of ground motion on slopes and mines. Details of the results obtained from refraction surveys at selected sites in the San Juan Basin (Gasbuggy Site) and Piceance Creek Basin (Rulison Site) are presented in Appendix A. Results of an Amplitude Amplification Study utilized in the ground motion predictions are presented in Appendix B.

The analyses leading to these predictions have been performed utilizing both empirical data and theoretical models. These techniques are limited in certain respects, and corresponding limitations are imposed on the confidence in the predictions. Explanations are provided in the text to indicate the source of empirical data and the assumptions that have been made in their interpretation.

This page intentionally left blank

Chapter 2

SUMMARY OF PREDICTIONS

TABLE 2-1
SUMMARY OF PREDICTIONS OF CLOSE-IN EFFECTS

Prediction	Maximum Yield	Design Yield
Cavity Radius	102±20 feet	90±18 feet
Cracking Radius	440-660 feet	390-580 feet
Radius of Gamma Radioactivity		
Above W.P.	160-280 feet	145-254 feet
Below W.P.	110-178 feet	100-161 feet
Chimney Height	425±85 feet	376±75 feet

TABLE 2-2
PREDICTED PEAK RESULTANT VECTOR AMPLITUDES, 40 KT

LOCATION	DISTANCE (km)	ROCK TYPE*	ACCELERATION (g)	DISPLACEMENT (cm)	VELOCITY (cm/sec)
Holmes Mesa	6.2	H	6.0×10^{-1}	1.5×10^{0}	2.1×10^{1}
Morrisania Mesa	6.8	H	5.1×10^{-1}	1.3×10^{0}	1.8×10^{1}
Rulison	8.0	H	3.8×10^{-1}	8.7×10^{-1}	1.3×10^{1}
Grand Valley	10.3	H	2.2×10^{-1}	5.5×10^{-1}	7.8×10^{0}
Anvil Points	12.7	H	1.6×10^{-1}	3.9×10^{-1}	5.5×10^{0}
Collbran	18.6	H	7.2×10^{-2}	2.0×10^{-1}	2.6×10^{0}
Rifle	20.5	H	5.9×10^{-2}	1.7×10^{-1}	2.2×10^{0}
DeBeque	24.2	H	4.4×10^{-2}	1.3×10^{-1}	1.6×10^{0}
Silt	29.8	H	2.9×10^{-2}	8.9×10^{-2}	1.1×10^{0}
Rio Blanco	37.2	H	1.9×10^{-2}	6.2×10^{-2}	7.5×10^{-1}
Glenwood Springs	56.5	H	8.6×10^{-3}	2.9×10^{-2}	3.5×10^{-1}
Grand Junction	65.0	H	6.4×10^{-3}	2.3×10^{-2}	2.6×10^{-1}
Meeker	69.5	H	5.8×10^{-3}	2.0×10^{-2}	2.3×10^{-1}
Delta	75.0	H	4.8×10^{-3}	1.7×10^{-2}	2.0×10^{-1}
Montrose	103	H	2.6×10^{-3}	9.6×10^{-3}	1.1×10^{-1}
Craig	128	H	1.7×10^{-3}	6.6×10^{-3}	7.2×10^{-2}
Denver	256	A	1.3×10^{-3}	7.1×10^{-3}	6.4×10^{-2}
Salt Lake City	367	A	7.4×10^{-4}	4.1×10^{-3}	3.5×10^{-2}

*H = Hard Rock (All locations in the Piceance Creek Basin have been designated "Hard Rock" to be consistent with the prediction method described in Chapter 5)

A = Alluvium (Stations situated on alluvium outside the Piceance Creek Basin)

TABLE 2-3

PREDICTED PEAK RESULTANT VECTOR AMPLITUDES, 60 KT

LOCATION	DISTANCE (km)	ROCK TYPE*	ACCELERATION (g)	DISPLACEMENT (cm)	VELOCITY (cm/sec)
Holmes Mesa	6.2	H	8.0×10^{-1}	1.9×10^{0}	2.8×10^{1}
Morrisania Mesa	6.8	H	7.0×10^{-1}	1.7×10^{0}	2.3×10^{1}
Rulison	8.0	H	5.0×10^{-1}	1.3×10^{0}	1.8×10^{1}
Grand Valley	10.3	H	2.9×10^{-1}	7.8×10^{-1}	1.1×10^{1}
Anvil Points	12.7	H	2.0×10^{-1}	5.6×10^{-1}	7.4×10^{0}
Collbran	18.6	H	9.7×10^{-2}	2.9×10^{-1}	3.6×10^{0}
Rifle	20.5	H	7.9×10^{-2}	2.4×10^{-1}	3.0×10^{0}
DeBeque	24.2	H	5.8×10^{-2}	1.8×10^{-1}	2.2×10^{0}
Silt	29.8	H	3.9×10^{-2}	1.3×10^{-1}	1.5×10^{0}
Rio Blanco	37.2	H	2.5×10^{-2}	8.8×10^{-2}	9.9×10^{-1}
Glenwood Springs	56.5	H	1.1×10^{-2}	4.1×10^{-2}	4.5×10^{-1}
Grand Junction	65.0	H	8.5×10^{-3}	3.3×10^{-2}	3.5×10^{-1}
Meeker	69.5	H	7.6×10^{-3}	2.9×10^{-2}	3.1×10^{-1}
Delta	75.0	H	6.5×10^{-3}	2.6×10^{-2}	2.7×10^{-1}
Montrose	103	H	3.4×10^{-3}	1.4×10^{-2}	1.5×10^{-1}
Craig	128	H	2.2×10^{-3}	9.9×10^{-3}	9.8×10^{-2}
Denver	256	A	1.6×10^{-3}	9.8×10^{-3}	7.9×10^{-2}
Salt Lake City	367	A	8.9×10^{-4}	5.5×10^{-3}	4.2×10^{-2}

*H = Hard Rock (All locations in the Piceance Creek Basin have been designated "Hard Rock" to be consistent with the prediction method described in Chapter 5)

A = Alluvium (Stations situated on alluvium outside the Piceance Creek Basin)

TABLE 2-4

PREDICTED PEAK HORIZONTAL ACCELERATIONS AT SELECTED LOCATIONS

LOCATION	DISTANCE (km)	PEAK HORIZONTAL ACCELERATION, g	
		40 kt	60 kt
Holmes Mesa	6.2	2.8×10^{-1}	4.0×10^{-1}
Morrisania Mesa	6.8	2.4×10^{-1}	3.4×10^{-1}
Rulison	8.0	1.8×10^{-1}	2.6×10^{-1}
Grand Valley	10.3	1.2×10^{-1}	1.7×10^{-1}
Collbran	18.6	4.4×10^{-2}	6.5×10^{-2}
Rifle	20.5	3.8×10^{-2}	5.3×10^{-2}
DeBeque	24.2	2.8×10^{-2}	4.1×10^{-2}
Silt	29.8	2.0×10^{-2}	2.9×10^{-2}
Harvey Gap Dam	33.0	1.7×10^{-2}	2.4×10^{-2}
Glenwood Springs	56.5	6.8×10^{-3}	9.7×10^{-3}
Grand Junction	65.0	5.5×10^{-3}	7.8×10^{-3}
Delta	75.0	4.3×10^{-3}	6.2×10^{-3}
Montrose	103.0	2.4×10^{-3}	3.5×10^{-3}

TABLE 2-5

PEAK RESULTANT VECTOR AMPLITUDES (60 KT) AT LOCATIONS HIGHLY SUSCEPTIBLE TO NATURAL ROCK FALLS

LOCATION	DISTANCE (km)	ACCELERATION (g)	DISPLACEMENT (cm)	VELOCITY (cm/sec)
Vega Dam Road	20	6.3×10^{-2}	2.1×10^{-1}	2.4×10^{0}
Road to Oil Shale Corp.	24	5.9×10^{-2}	1.9×10^{-1}	2.3×10^{0}
Route 65-330 Intersection	29	4.0×10^{-2}	1.3×10^{-1}	1.6×10^{0}
~1 mile east of Silt	30	3.5×10^{-2}	1.1×10^{-1}	1.3×10^{0}
DeBeque Pass	34	3.1×10^{-2}	1.0×10^{-1}	1.2×10^{0}
Plateau Creek Canyon	34	3.1×10^{-2}	1.0×10^{-1}	1.2×10^{0}
Glenwood Canyon	65	8.5×10^{-3}	3.3×10^{-2}	3.5×10^{-1}

Note: It is anticipated that ground motion from the Rulison event will increase the probability of rock falls making rail and highway traffic through the above areas hazardous at shot time.

TABLE 2-6

PEAK RESULTANT VECTOR AMPLITUDES (60 KT) AT CLOSE-IN DAM SITES

DAM SITE	DISTANCE (km)	ACCELERATION (g)	DISPLACEMENT (cm)	VELOCITY (cm/sec)
Battlement	4.8 (Slant)	1.3×10^{0}	3.1×10^{0}	3.3×10^{1}
Watson	6.3 (Slant)	7.9×10^{-1}	1.9×10^{0}	2.7×10^{1}
McCurry	8.2 (Slant)	4.6×10^{-1}	1.2×10^{0}	1.6×10^{1}
Vega	23	6.3×10^{-2}	2.1×10^{-1}	2.4×10^{0}
Harvey Gap	33	3.3×10^{-2}	1.1×10^{-1}	1.3×10^{0}

TABLE 2-7

PEAK ACCELERATIONS NEAR SURFACE ZERO

Peak acceleration caused by initial signal	1-1/2 - 4-1/2 g
Peak acceleration caused by spall	2 - 15 g

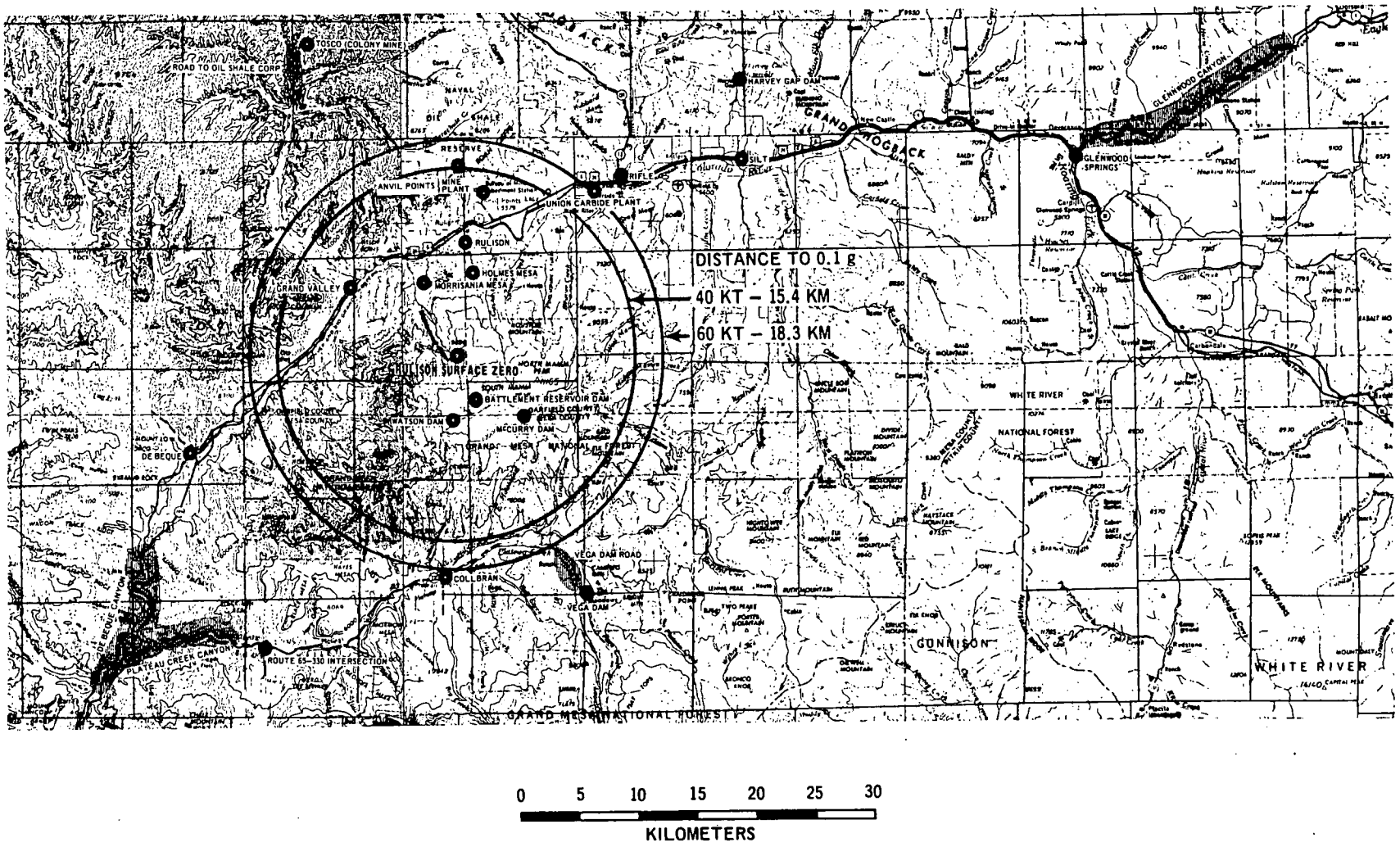

Figure 2-1. Area Map Showing Predicted Distances to 0.1 Accelerations of g

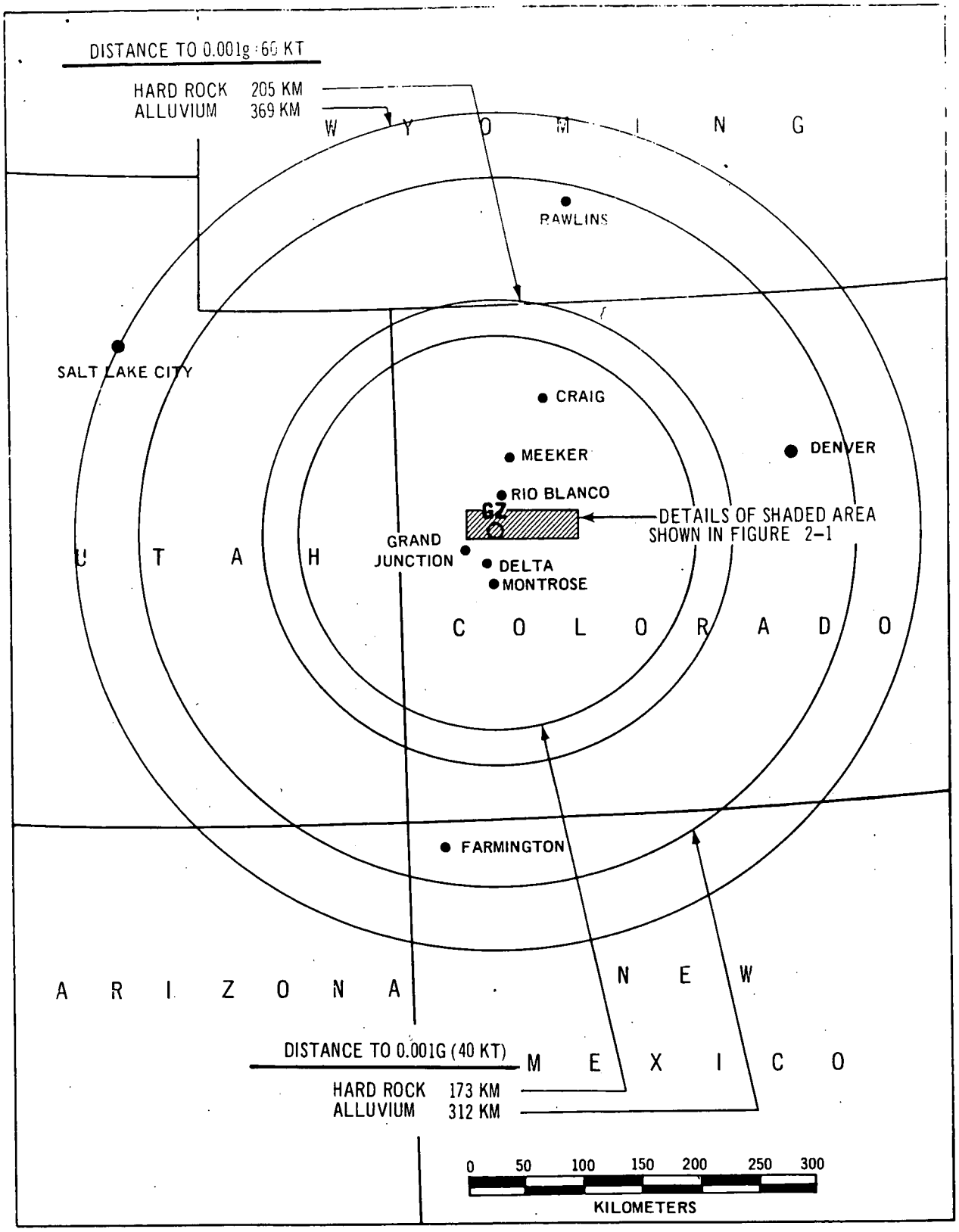

Figure 2-2. Area Map Showing Predicted Distances to 0.001 Accelerations of g

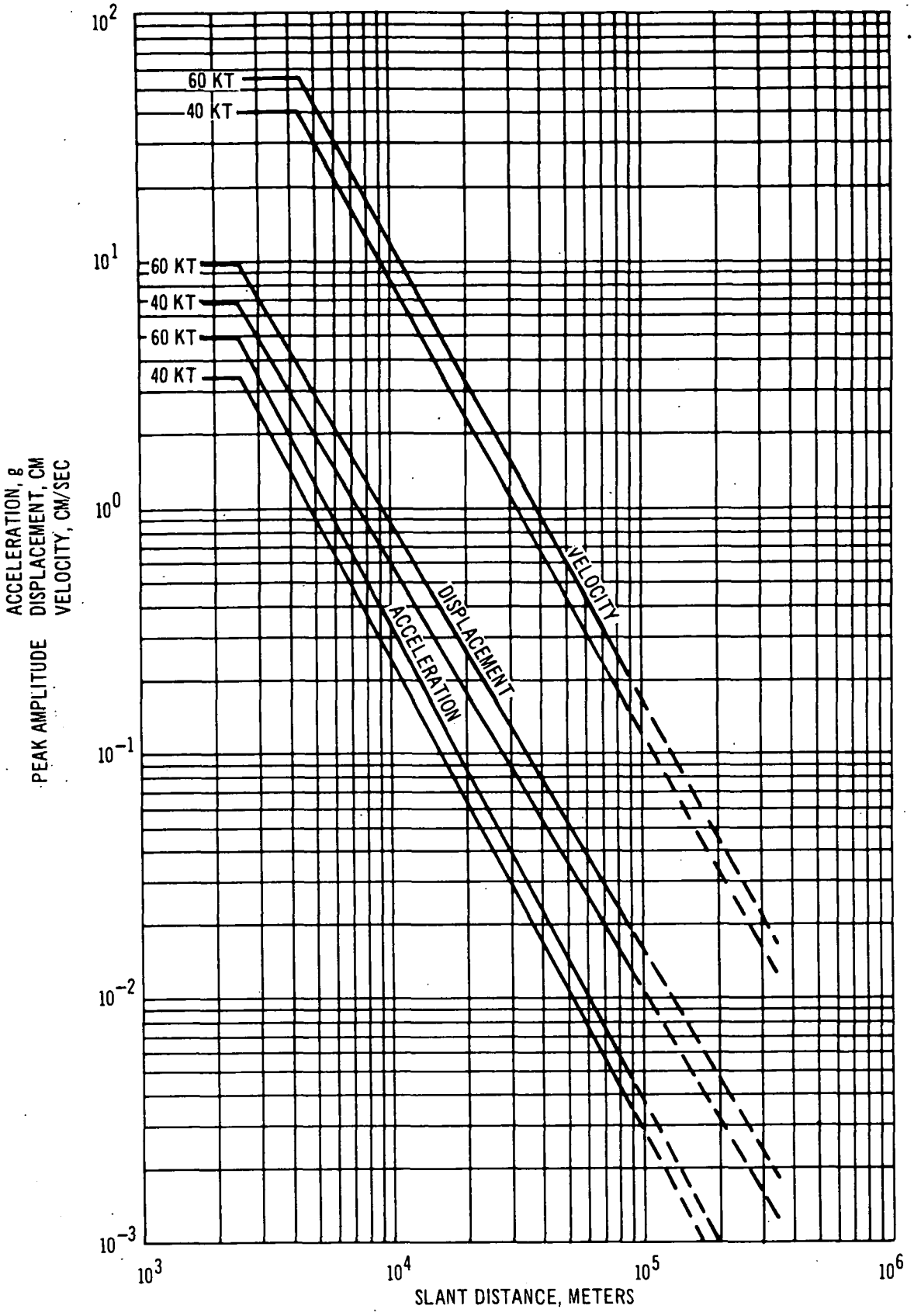

Figure 2-3. Predicted Peak Particle Resultant Vector Amplitudes for Locations on Hard Rock

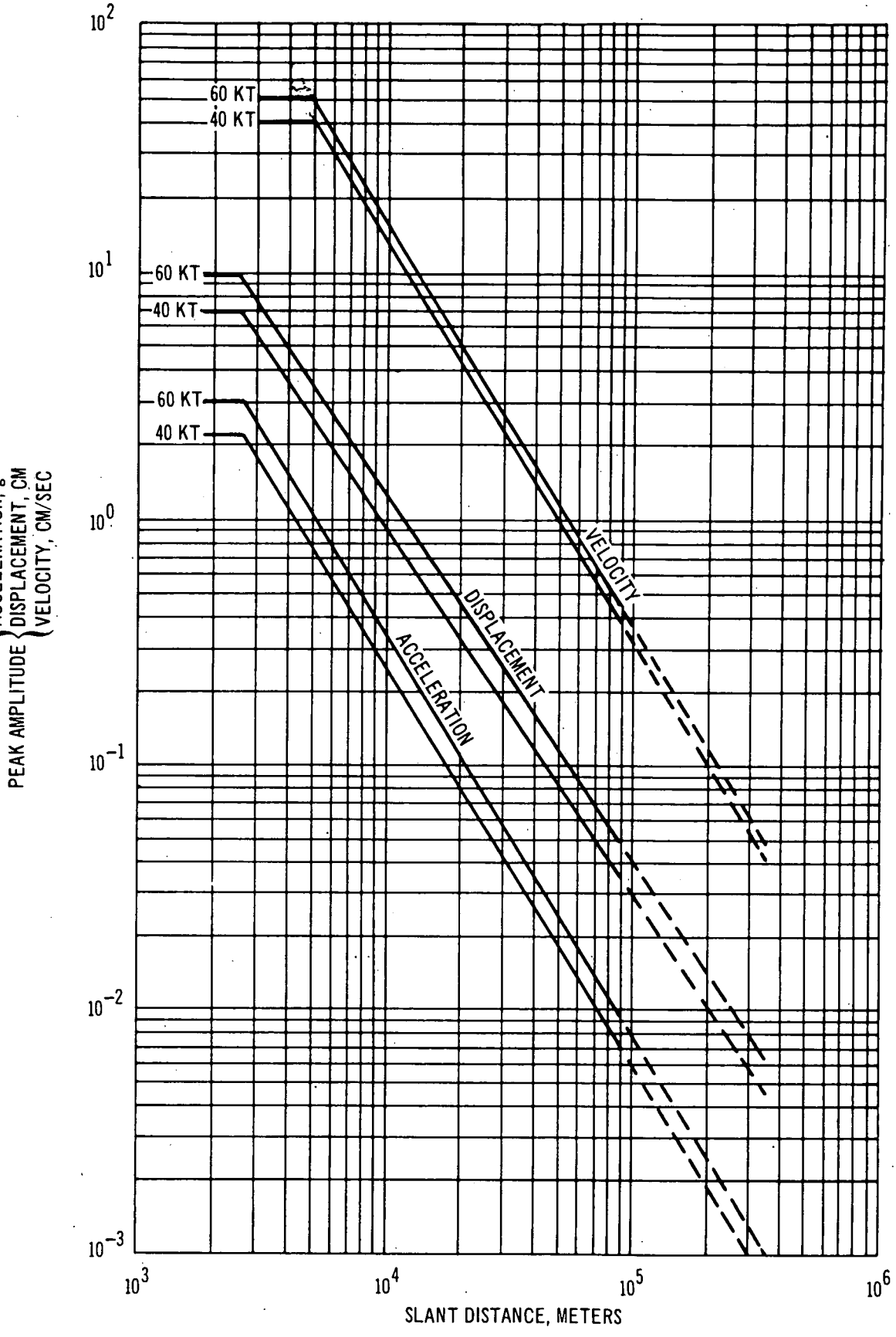

Figure 2-4. Predicted Peak Particle Resultant Vector Amplitudes for Locations on Alluvium

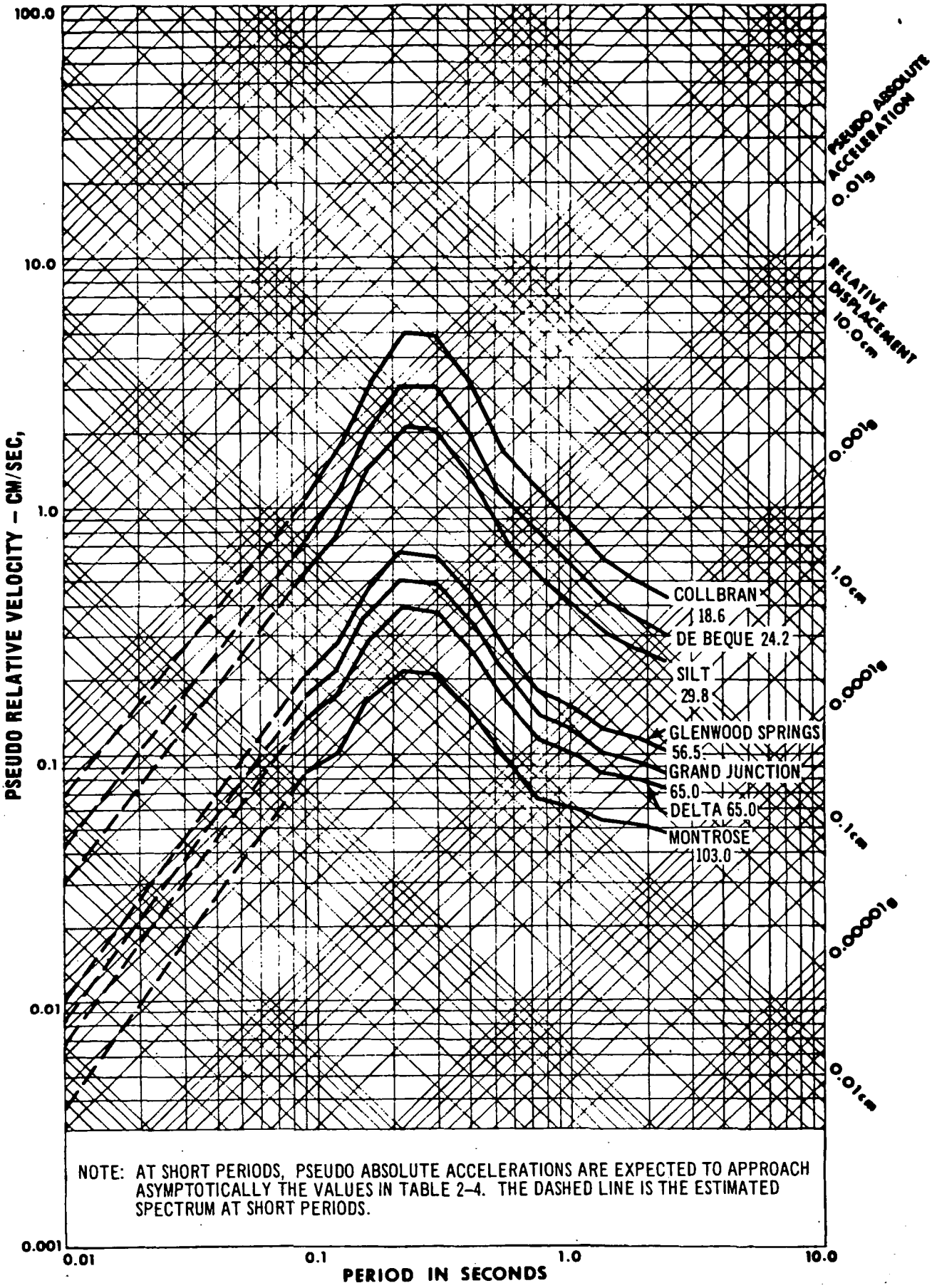

Figure 2-5. Predicted 5% PSRV Spectra, Rulison, 40 kt

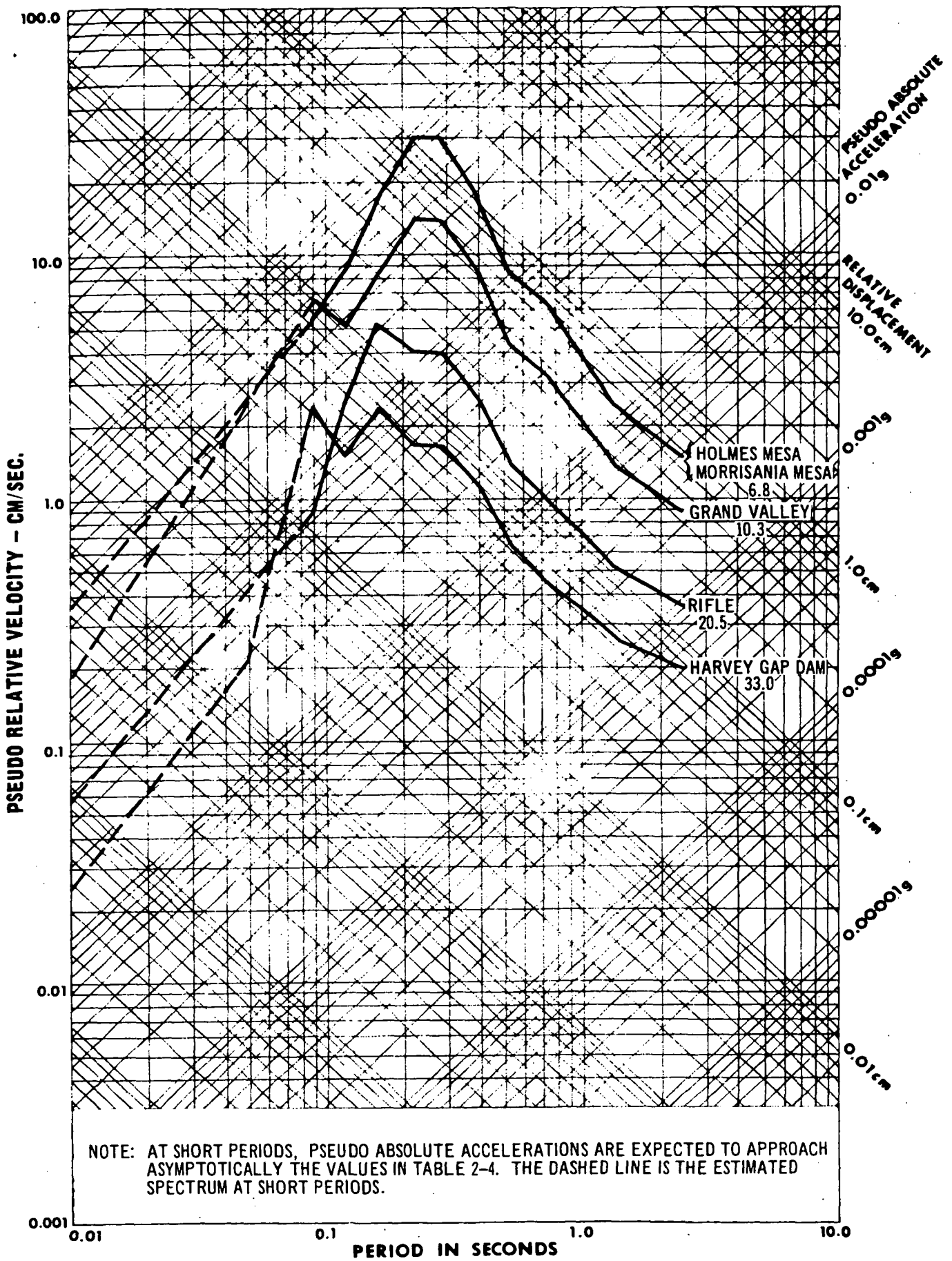

Figure 2-6. Predicted 5% PSRV Spectra, Rulison, 40 kt

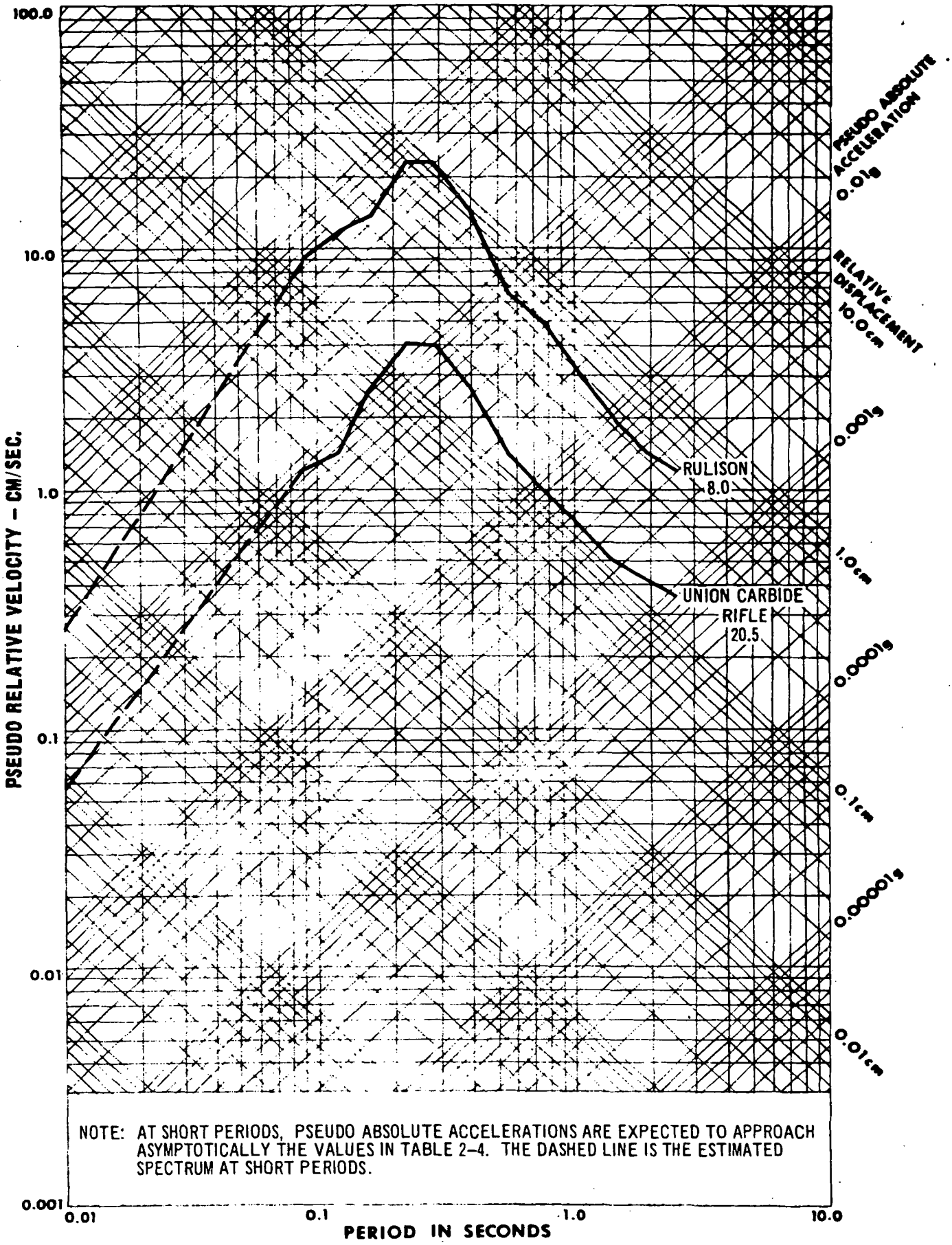

Figure 2-7. Predicted 5% PSRV Spectra, Rulison, 40 kt

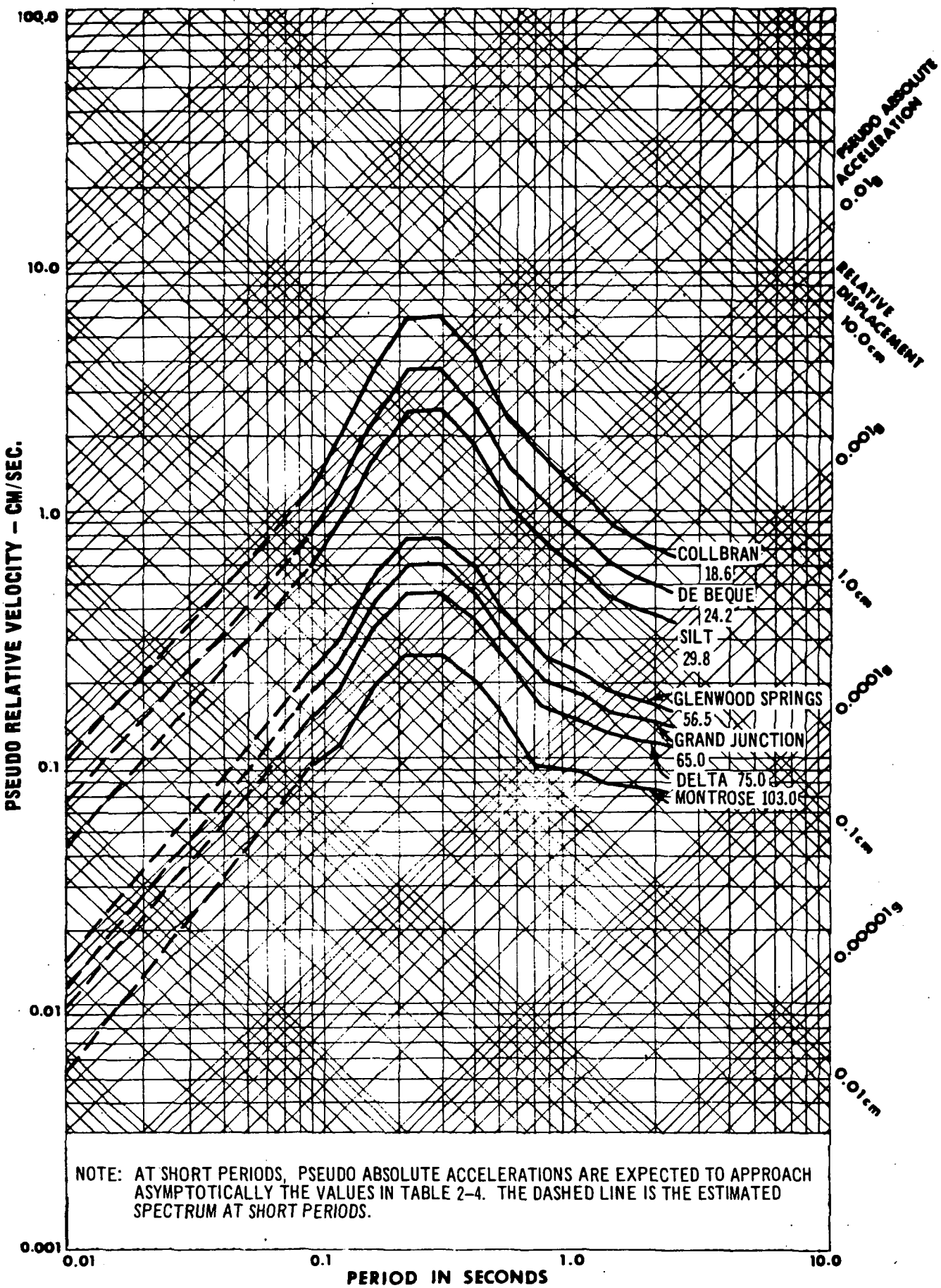

Figure 2-8. Predicted 5% PSRV Spectra, Rulison, 60 kt

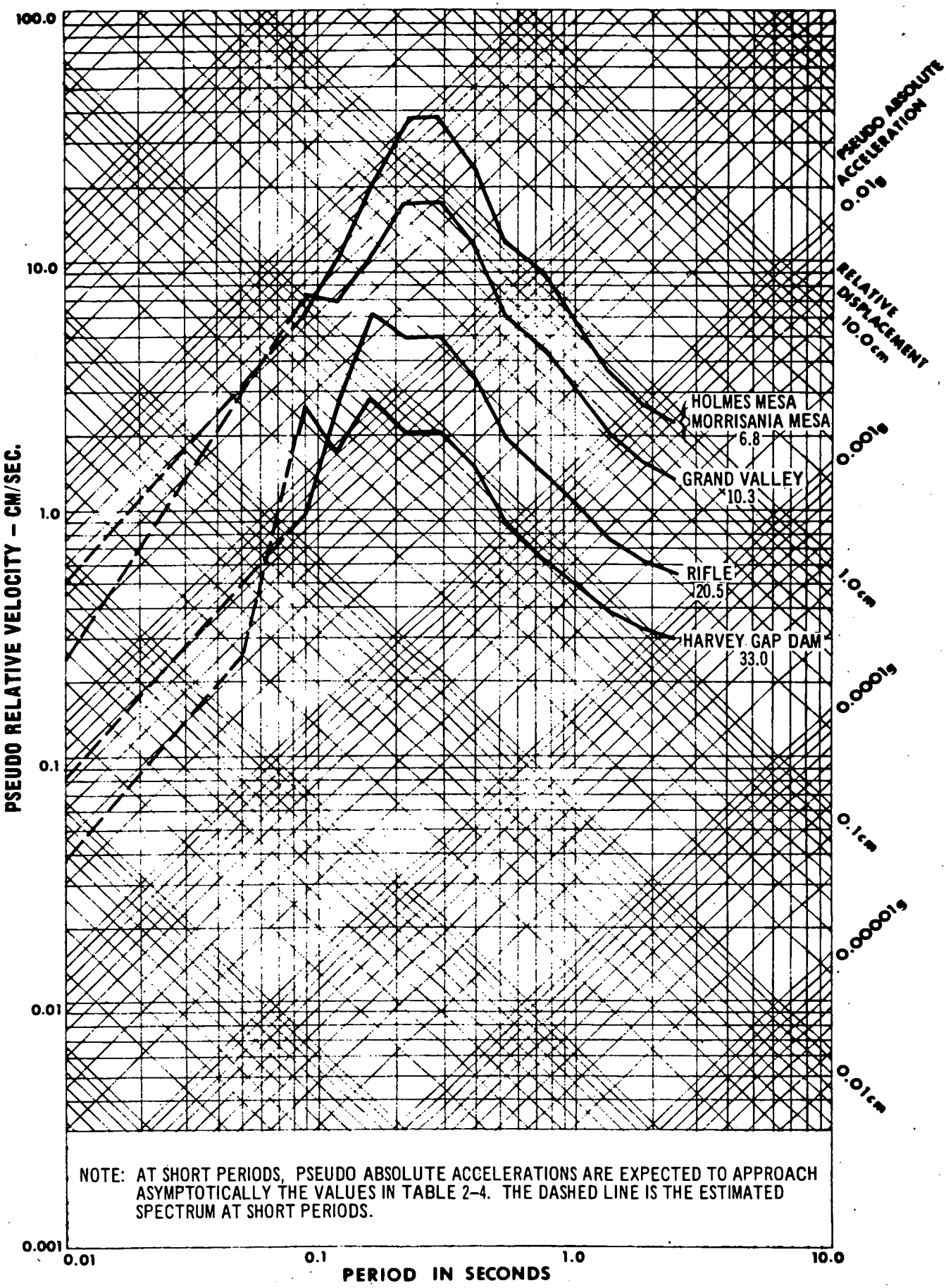

Figure 2-9. Predicted 5% PSRV Spectra, Rulison, 60 kt

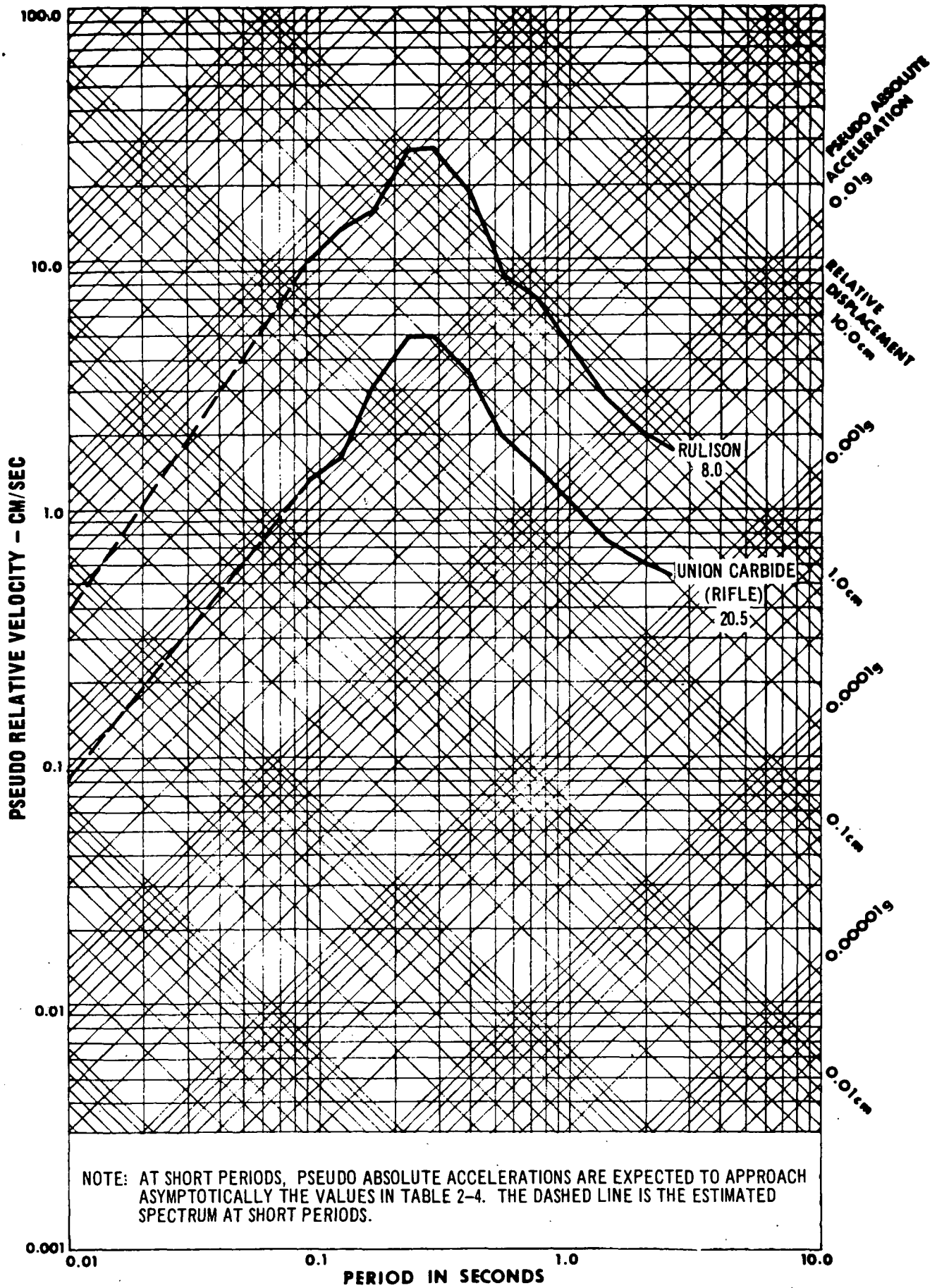

Figure 2-10. Predicted 5% PSRV Spectra, Rulison, 60 kt

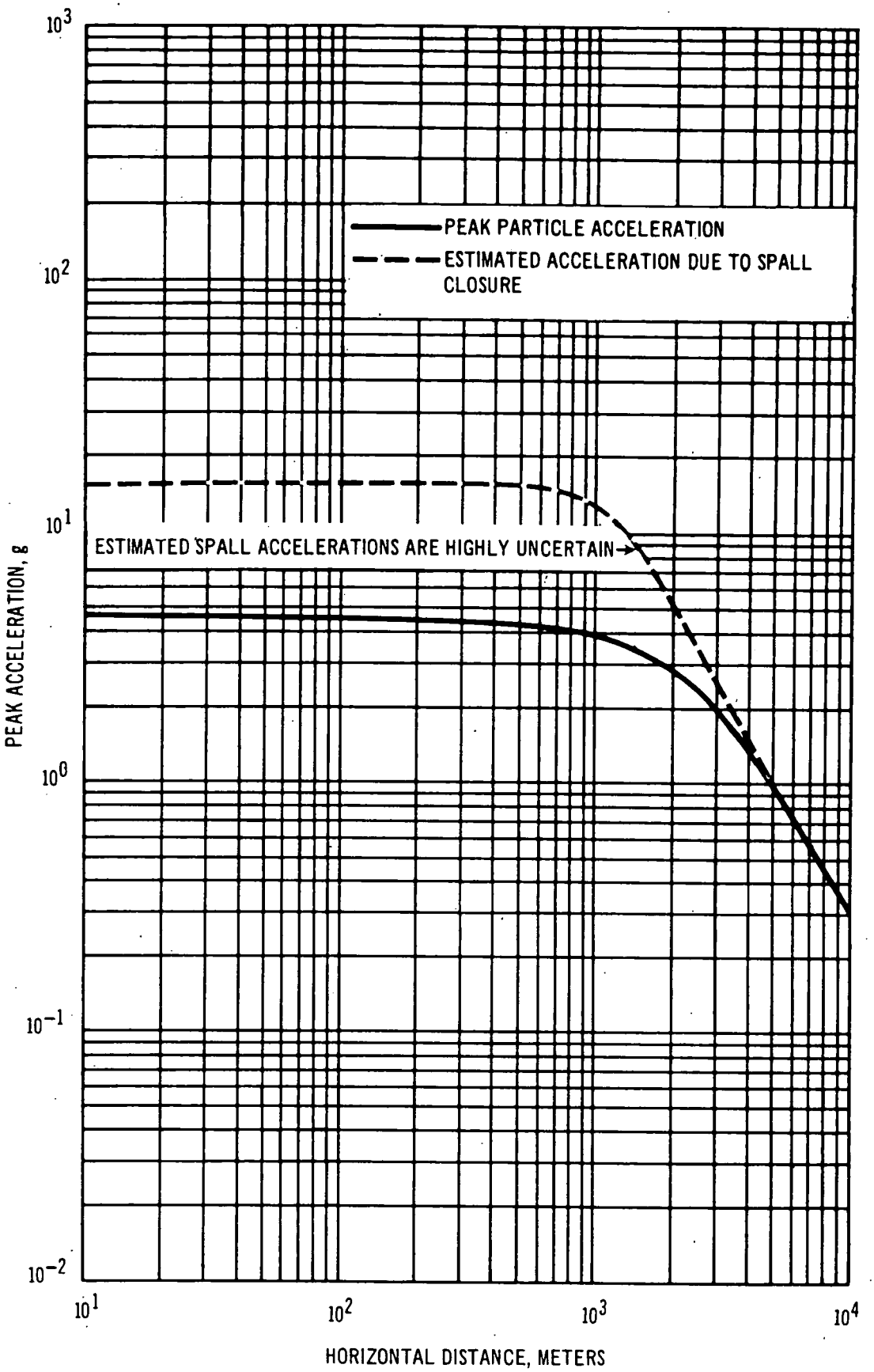

Figure 2-11. Close-In Peak Resultant Vector Particle Accelerations Including Peaks Caused by Spall Closure, Rulison, 60 kt

Chapter 3
GEOLOGIC ENVIRONMENT

3.1 LOCATION AND TOPOGRAPHY

The Rulison Project is located in northwestern Colorado in the Rulison gas field of the Piceance Creek Basin (see Figure 3-1). The drill hole is collared at an elevation of about 8,200 feet in the upper reaches of Battlement Creek on the north slope of Battlement Mesa in south-central Garfield County. The creek valley opens to the north-northwest and is bound on the east, south, and west by slopes rising to above 9,600 feet (Reference 3.1).

3.2 STRATIGRAPHY AND LITHOLOGY

The Rulison gas field is on the southwest flank of the Piceance Creek Basin (see Figure 3-2). Upper Cretaceous beds in this area are relatively flat-lying, dipping toward the northeast at a rate of 150 feet per mile (Reference 2.1). Beds of Tertiary age are also relatively flat-lying.

Table 3-1 is a general sequence of the rocks present at the Rulison site. The drill hole lies at the northern edge of a basalt slump block which forms most of the surface outcrop of Battlement Mesa to the south (reference 3.2). At a depth of 1,700 feet, in the Rulison exploratory well, is the base of the Green River Formation, a series of dark colored oil shales, marlstones, and sandstones. Underlying this and continuing to a depth of 6,134 feet are the impermeable Wasatch and Fort Union shales and siltstones. At the base of the Tertiary, the Ohio Creek Formation was encountered between the Fort Union shales and the top of the Upper Cretaceous, the Mesaverde Formation, at 6,188 feet (Reference 2.1). The Mesaverde Formation consists of shales with interspersed lenticular sandstones of limited areal extent which are the gas-bearing formations of the Rulison Field. This formation contains several hundred feet of potential gas reservoirs in the intermittent sand-shale stringers (Reference 3.1). The Mesaverde Formation ranges in thickness from 2,500 to 4,000 feet, and is underlain by the Mancos Formation, a sequence of Lower Cretaceous shales and sandstones having a combined thickness of 2,500 feet (Reference 2.1).

3.3 PHYSICAL PROPERTIES

The following representative physical properties of the event medium are averaged from other wells in the Rulison Field (Reference 2.1):

Median Porosity	9.7%
Average Water Saturation	45.0%
Average Gas Saturation	~54%
Average Oil Saturation	<1%
Average Overburden Density	2.35 gm/cc

TABLE 3-1
GENERAL SEQUENCE OF ROCKS OVERLYING THE RULISON GAS-BEARING FORMATION (MESAVERDE)
(ADAPTED FROM REFERENCE 2.1)

SYSTEM AND PERIOD	"FORMATIONS"	GENERAL LITHOLOGY OF PICEANCE CREEK BASIN	DEPTH AT HOLE R-EX
Quaternary	"Recent"	Low Terrace, flood plain, and alluvial deposits	
	"Pleistocene"	Terrace and fan sand and gravel, pediment gravel, colluvium, mudflow, and solifluction deposits	
Tertiary	(?)	Basalt flows underlain by variegated claystones and gravel	
	Green River	Oil shales, marlstones, and sandstones (dark color)	
	Wasatch	Bright colored clays and shale with minor sandstone	1,700 ft.
	Fort Union	Brown-gray shale and coal	6,134 ft.
	Ohio Creek	Sandstone and conglomerate	6,188 ft.
Cretaceous (Upper)	Mesaverde	Shale - sandstone	Shot Point 8,442.5 ft.

3.4 STRUCTURE

As previously reported, bedding in the Piceance Creek Basin is essentially parallel and displays a dip of approximately 150 feet per mile to the northeast or center of the Basin. In the immediate area of the emplacement hole, stereo aerial coverage disclosed lineations which were subsequently examined by field reconnaissance. Most of the lineations were found to be related to well-developed joint-sets in the area; others were associated with slide margins and topographically controlled vegetation changes. No displacements or traces of faulting were found (Reference 2.1).

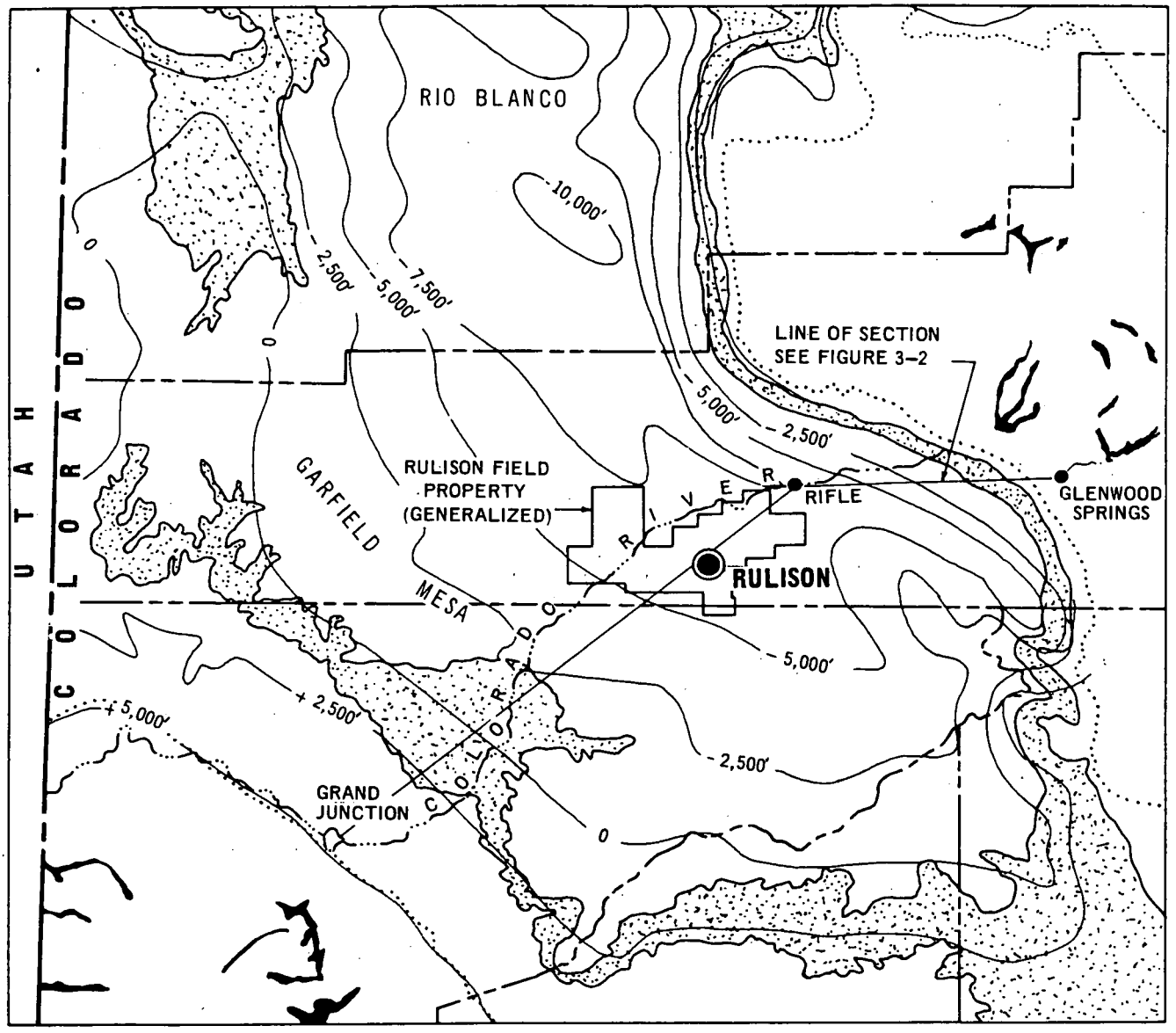

Figure 3-1. Regional Geological and Structural Map of the Piceance Creek Basin, Northwestern Colorado, showing the Rulison Site

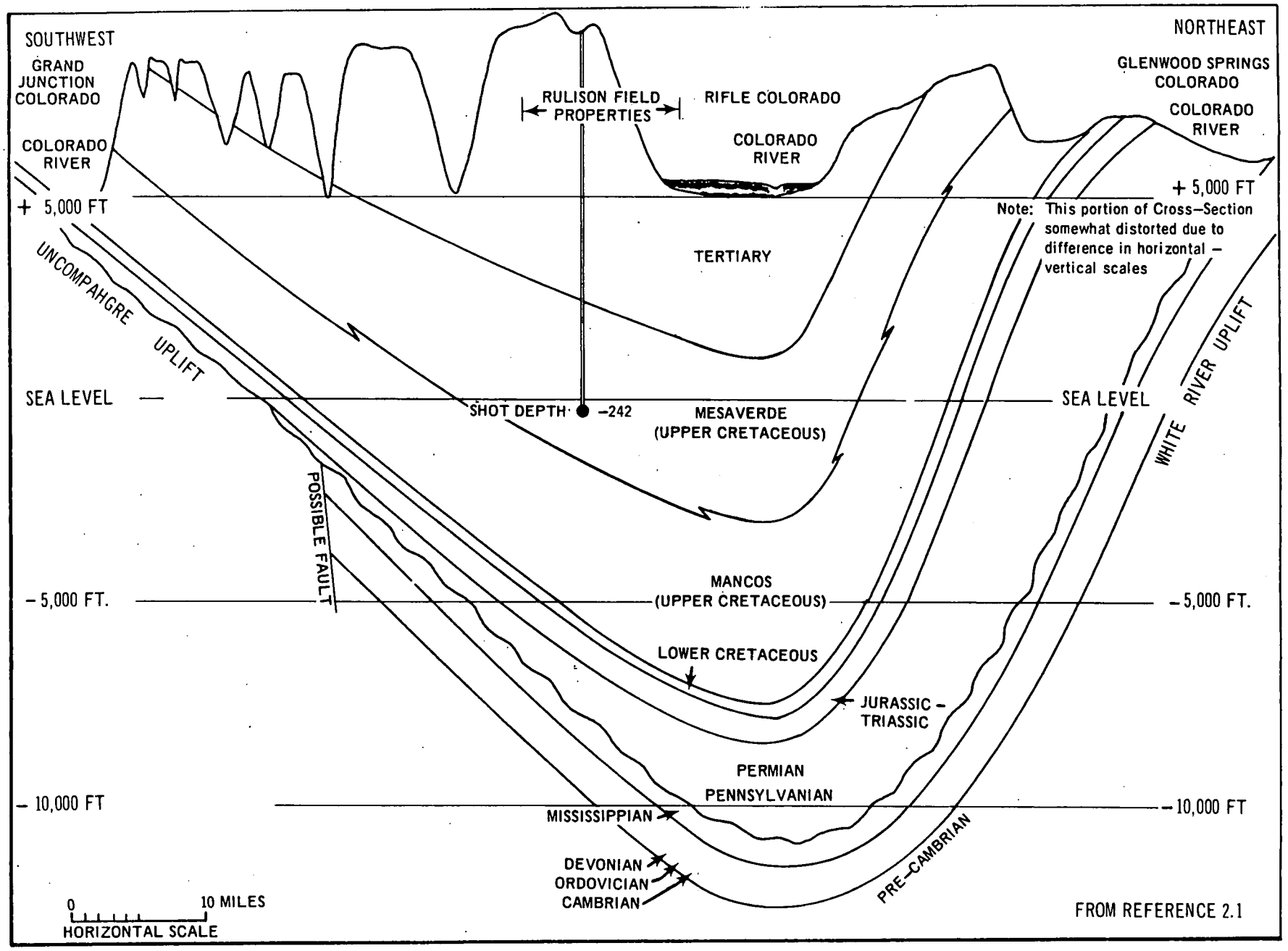

Figure 3-2. Generalized Cross-Section Across the Piceance Creek Basin, Colorado

3.5 HYDROLOGY

Most of the precipitation in the Rulison area is carried into the Colorado River by small streams or underflows in the alluvial fill of small valleys. A few springs may be present where the underflow is deflected to the surface by impermeable bedrock. Some inhabitants near the Rulison site obtain water from shallow wells drilled into the alluvium or from cisterns and ponds fed by creeks or springs, some of which originate in the Battlement Creek drainage area (see Section 3.1).

Some sandy, water-bearing zones of the Green River Formation occur at elevations greater than 6,600 feet above sea level and are remote from permanent habitation.

The Wasatch Formation, underlying the Green River, is relatively impermeable and probably very little ground water movement occurs in this medium (Reference 2.1).

"Hydrologic tests on the Rulison exploratory hole indicated that little or no water occurs in the Ohio Creek Conglomerate and Mesaverde Group which are the stratigraphic units most likely to yield water to the hole. Six depth intervals, beginning at 6,129 feet and ending at 8,018 feet, were tested. Pressures recorded during the testing of the individual zones indicated little or no fluid entry while the test tool was open." (Reference 3.3).

3.6 SUMMARY

In general terms, the Piceance Creek Basin of Colorado is geologically similar to the San Juan Basin of New Mexico where a similar experiment, called "Gasbuggy," took place. Essentially flat-lying beds of shales, siltstones, and sandstones predominate in the geologic columns at both sites. The topography close to Rulison surface zero is characterized by mud slumps, mud slides, and unconsolidated deposits which create more complex relief features than encountered at the Gasbuggy site.

Refraction surveys show that the near surface layers at selected Rulison and Gasbuggy locations have similar thicknesses and compressional velocities (see Appendix A). The surface layer at Rulison locations ranged from 3-25 feet in thickness with velocities between 1,000 and 1,470 ft/sec. At the Gasbuggy sites, the thicknesses varied from 10 to 94 feet and the velocity from 1,050 to 2,450 ft/sec.

This page intentionally left blank

Chapter 4
PREDICTIONS OF CLOSE-IN EFFECTS

The following sections provide the basis for the predictions of cavity radius, radius of cracking, radius of gamma radioactivity, and height of chimney presented in Chapter 2. Predictions of these and other effects have been made for the maximum yield of 60 kt and the design yield of 40 kt. In this section, only the calculations for the maximum yield are shown. The design yield predictions were made in an identical manner.

4.1 RADIUS OF CAVITY

When an underground nuclear explosion takes place, the energy released heats the surrounding earth material enough to vaporize some of the material. The explosion thus creates a "vaporization cavity" filled with gas at a very high pressure and temperature. This gas then expands until the forces acting on the cavity are in balance. The cavity is then at its maximum radius.

The final size of the cavity formed by an underground nuclear explosion depends on many factors. The two most important factors are the size or yield of the explosion and the geologic medium in which the explosion takes place.

The Rulsion event will be executed at a depth of 8,442.5 feet in the Mesaverde Formation in the Piceance Creek Basin of Northwest Colorado. The geology of the Rulison site is discussed in Chapter 3. The Gasbuggy event (Reference 4.1) was executed at a depth of 4,240 feet in the Lewis Shale Formation in the San Juan Basin of New Mexico. The geologic environment of the Gasbuggy detonation appears to be very similar to the medium surrounding Rulison. Therefore, the predictions of the cavity radii for Rulison are based on the Gasbuggy experience. The 26 kt Gasbuggy explosion formed a cavity with a radius of approximately 80 feet in shale and sandstone (Reference 4.2).

A multiple regression and statistical analysis of post-shot cavity radius data from 107 underground nuclear detonations showed that cavity radii for events in tuff and alluvium could be predicted by an equation of the form

$$R = K\, W^{0.286} \qquad (4\text{-}1)$$

where R is the cavity radius in feet, K is a constant and W is the event yield in kilotons. The value of K depends on the geologic environment of the detonation.

From equation 4-1, the cavity radii for two events in the same geologic medium are related by the equation

$$R_1 = R_2\left(\frac{W_1}{W_2}\right)^{0.286} \tag{4-2}$$

where R and W are defined above and the subscripts denote two different detonations.

Since the geologic environments of Rulison and Gasbuggy are similar, the cavity radius for Rulison is predicted using equation 4-2 where R_2 is taken as the Gasbuggy cavity radius and W_1 and W_2 are the yields in kilotons for Rulison and Gasbuggy, respectively. For the maximum Rulison yield of 60 kt the cavity radius is calculated to be

$$R = (80)\left(\frac{60}{26}\right)^{0.286} = 102 \text{ feet}$$

Experience at Nevada Test Site indicates that the standard error of estimate for predicting cavity radius is about 20 percent. Although it is uncertain whether such NTS experience is directly applicable to the Rulison event, a standard error of estimate of 20 percent is considered reasonable for the Rulison cavity radius prediction. On this basis, the Rulison cavity radius is predicted to be 102±20 feet for a yield of 60 kt.

It should be noted that the Rulison event will be executed at a greater depth than any previous underground nuclear detonation. Several theoretical descriptions of cavity formation indicate that the depth of burial of the explosion influences the final cavity radius. The indicated influence of the depth on the cavity radius is small, however, and is generally insignificant compared with the uncertainty in the predictions due to variations in the physical properties of the geologic environment. It is noted however, that the theoretical effect of depth on the Rulison cavity radius would make the cavity slightly smaller than predicted above.

4.2 RADIUS OF CRACKING

An underground nuclear detonation creates a shock wave that travels outward from the vaporization cavity described in the previous section. This shock wave melts some of the earth material around the vaporization cavity and also produces cracks in the material out to some distance. The expansion of the vaporization cavity to its final size also contributes to the formation of a highly cracked zone around the cavity. Figure 4-1 illustrates, in a simplified fashion, the cavity and cracked region formed by an underground nuclear explosion.

Using the techniques described in Reference 4.3, it has been shown that the extent of radial fracturing for the Rainier event corresponds to a permanent radial strain of 0.8 percent in the medium. Applying the methods given in Reference 4.3 and assuming a 0.8 percent permanent radial strain as a cracking criterion, the outer limit of fracturing for tuff would be predicted to be 440 feet for a cavity radius of 102 feet.

Using the same procedure and applying a permanent radial strain criterion of 0.25 percent (Reference 4.4), the outer limit of cracking for granite would be predicted to be 660 feet for a cavity radius of 102 feet.

Since the shale and sandstone surrounding the Rulison explosion probably have properties similar to those found at Gasbuggy (Reference 4.1) and between those of granite and tuff, a cracking radius of 440-660 feet is predicted for Rulison at the maximum yield of 60 kt.

4.3 RADIUS OF GAMMA RADIOACTIVITY

An underground nuclear detonation produces gamma radioactivity. With the formation of the cavity and the cracked region surrounding the explosion, some of this radioactivity passes into the earth.

Studies of events at the Nevada Test Site indicate that gamma radioactivity from an underground nuclear explosion does not extend to equal distances in all directions from the detonation point. The radius of gamma radioactivity for Rulison is predicted by applying the results of these studies and assuming that the radius and its associated standard error of estimate at Rulison will approximate that predicted for an event of similar yield at NTS. On the above basis, the radius of gamma radioactivity for Rulison is predicted to be between 160 and 280 feet above and 110 and 178 feet below the detonation point.

4.4 HEIGHT OF CHIMNEY

Generally, within a short time after the explosion, the cavity collapses. This collapse progresses upward to form a chimney. The chimney stops growing when:

1) the volume of the original cavity has been distributed between the chimney rubble.
2) the arch forming the top of the chimney can withstand the weight of the earth materials over it.
3) the chimney intersects the surface.

The chimney formed by an underground nuclear explosion is illustrated in Figure 4-2.

The height of the chimney can be predicted using the equation

$$H = \frac{(2/3)\ R\ (N+1)}{(N-1)} \qquad (4\text{-}3)$$

where H is the chimney height in feet, R is the predicted cavity radius in feet and N is the bulking factor (i.e., the ratio of the volume assumed by a given quantity of earth material after collapse to the original volume of the material). The bulking factor reflects the disorderly packing of the chimney rubble.

The bulking factor, N, for chimney rubble may be calculated using the equation

$$N = \frac{V_{ch} + \frac{1}{2} V_c}{V_{ch} - \frac{1}{2} V_c} \qquad (4\text{-}4)$$

where V_{ch} is the volume of the chimney and V_c is the volume of the cavity.

Because the bulking factor is greatly influenced by the geologic environment of the chimney, N for Rulison was predicted on the basis of the experience at Gasbuggy.

Early post-shot data from the Gasbuggy event (Reference 4.2) indicate that the Gasbuggy chimney contained no apical void and had a radius of approximately 80 feet and a height of 333 feet. If it is assumed that the Gasbuggy chimney was cylindrical with the above dimensions, and that the cavity was spherical, the bulking factor for the chimney rubble is calculated from equation (4-4) to be 1.38.

Assuming a bulking factor of 1.38 for Rulison, the height of the chimney is predicted using equation (4-3). For R = 102 feet and N = 1.38,

$$H = \frac{(2/3)\,(102)\,(2.38)}{0.38} = 425 \text{ feet}$$

Taking into consideration the uncertainty in the cavity radius prediction (see Section 4.1), the Rulison chimney height is predicted to be 425±85 feet for a yield of 60 kt.

It should be noted that since the prediction of chimney height involves the cavity radius, any influence of depth on the cavity radius (see Section 4.1) will affect the height of the chimney in a similar manner.

4.5 SURFACE SPALLING

When the elastic wave produced by the underground explosion reaches the surface above the detonation point and is reflected back into the earth, a horizontal separation of one or more surface layers of earth material may occur. This separation of layers is known as spalling.

Due to the depth of the Rulison explosion, spalling is not expected to be significant. Calculations based on experience at the Nevada Test Site indicate that if surface spalling occurs, it will extend only to a depth of approximately 65 feet (for further discussion of spalling see Section 6.3).

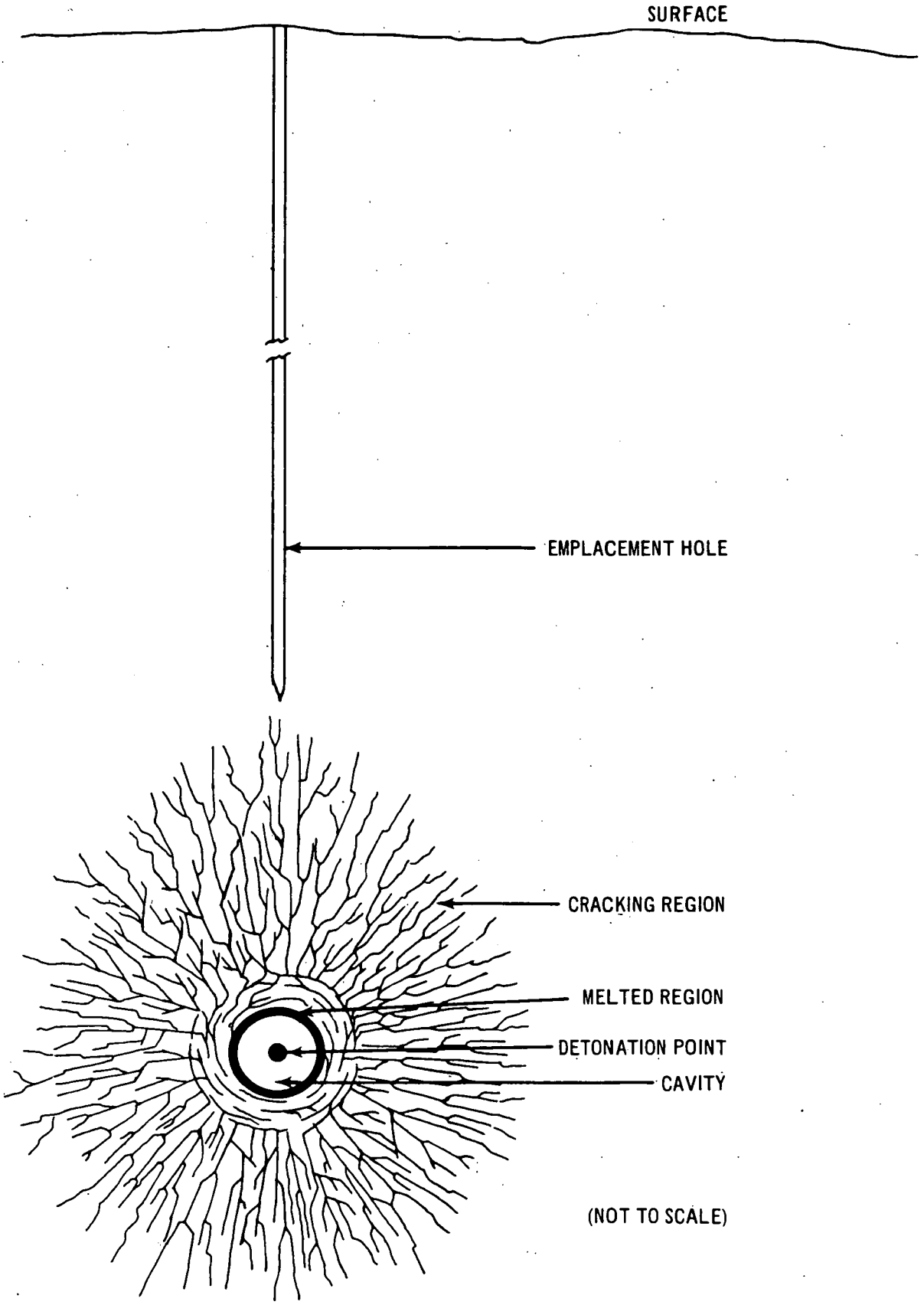

Figure 4-1. Diagrammatic Illustration of the Cavity and Cracked Region Formed by an Underground Nuclear Explosion

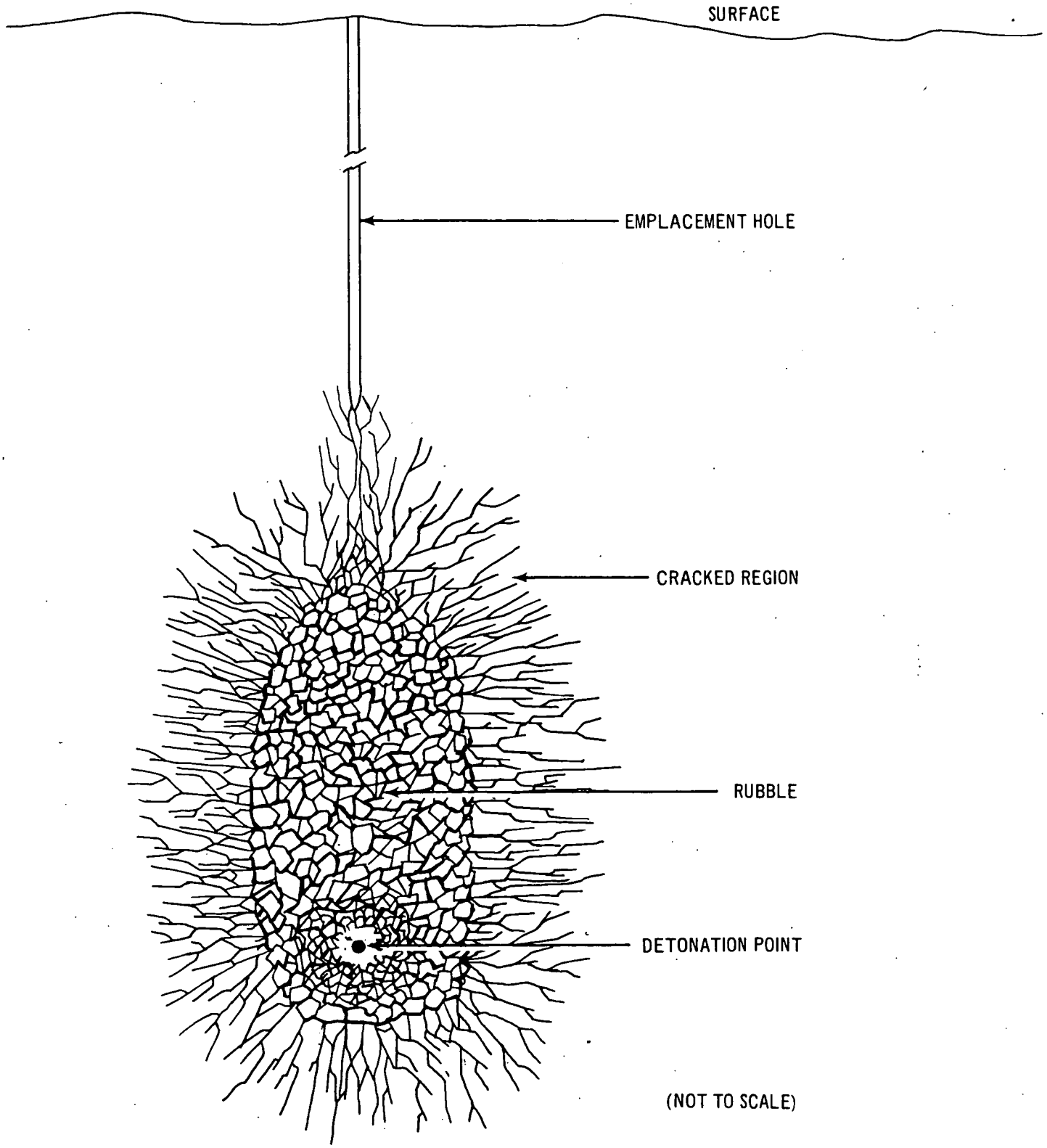

Figure 4-2. Diagrammatic Illustration of Chimney Produced by an Underground Nuclear Explosion

Chapter 5
SEISMIC PREDICTIONS

5.1 GENERAL

The following sections provide explanation of the methods used to make the ground motion predictions found in Chapter 2. These predictions are based on the assumption that ground motions from Rulison (Piceance Creek Basin) will be similar to those from Gasbuggy (San Juan Basin). The bases for this assumption are the similarity of the geologic environments in which each explosive is emplaced, the overburied nature of the explosive, and the generally similar nature of the ground motion amplification, as determined by refraction surveys and analytical amplification modeling.

5.2 PEAK RESULTANT VECTOR AMPLITUDE PREDICTIONS

Peak particle ground motion amplitude predictions were based on regression lines through Gasbuggy data. All Gasbuggy data were grouped together to provide the "hard rock" data sample, because peak motion data at Gasbuggy stations with thin alluvial cover did not differ significantly from data at adjacent hard rock stations.

A regression line expressing peak amplitude as a function of distance was derived from the total Gasbuggy data sample and scaled to the Rulison yields, using yield scaling exponents derived from NTS experience. These exponents are 0.66, 0.77 and 0.85 for acceleration, velocity, and displacement, respectively. (Reference 5.1). The equations thus derived were used to predict for locations of interest within the Piceance Creek Basin, regardless of alluvium cover, and are called hard rock equations to be consistent with Gasbuggy experience.

For locations of interest on alluvium outside the Piceance Creek Basin (Salt Lake City and Denver), prediction equations were derived by applying "distance dependent" amplification factors to the hard rock equations. The factors are such that the ratio between the Rulison alluvium and hard rock equations is the same, at any distance, as the ratio between NTS alluvium and hard rock equations. In this manner, the hard rock-alluvium relationship is kept consistent with statistically derived data from NTS.

The peak resultant vector amplitude prediction equations are:

Acceleration	40kt	60kt
Hard Rock Sites:	$a = 1.26 \times 10^{7} R^{-1.93}$	$a = 1.64 \times 10^{7} R^{-1.93}$
Alluvium Sites:	$a = 8.15 \times 10^{5} R^{-1.63}$	$a = 1.08 \times 10^{6} R^{-1.63}$

Velocity	40kt	60 kt
Hard Rock Sites:	$u = 2.30 \times 10^{8} R^{-1.86}$	$u = 3.14 \times 10^{8} R^{-1.86}$
Alluvium Sites:	$u = 4.78 \times 10^{7} R^{-1.64}$	$u = 5.78 \times 10^{7} R^{-1.64}$
Displacement		
Hard Rock Sites:	$d = 6.00 \times 10^{6} R^{-1.75}$	$d = 8.49 \times 10^{6} R^{-1.75}$
Alluvium Sites:	$d = 9.01 \times 10^{5} R^{-1.50}$	$d = 1.23 \times 10^{6} R^{-1.50}$

where:

a = peak resultant vector surface particle acceleration in g

u = peak resultant vector surface particle velocity in cm/sec

d = peak resultant vector surface particle displacement in cm

R = slant distance in meters

5.3 PREDICTED DISTANCES TO 0.1 g AND 0.001 g

These distances were predicted directly from the graphs in Chapter 2. The distances are shown in relation to surrounding communities in Figures 2-1 and 2-2.

5.4 PREDICTED PEAK HORIZONTAL PARTICLE ACCELERATIONS

Predicted peak horizontal particle accelerations (Table 2-4) were made in basically the same way as the peak vector particle motion, except that the regression line through Gasbuggy data was obtained by using the largest horizontal component of acceleration instead of the resultant vector. This equation was then scaled to the Rulison yield using the yield exponent of 0.66.

5.5 PSEUDO-RELATIVE VELOCITY (PSRV) PREDICTIONS

Three steps were used to predict the response spectra at points of interest within the Piceance Creek Basin. These steps are: 1) derivation of regression lines from the total Gasbuggy band-pass filter (BPF) data sample to express peak velocity for a particular frequency as a function of distance, 2) incorporation of a frequency-dependent depth of burial factor, and 3) incorporation of an amplification factor (at seven selected sites) based on results obtained from refraction surveys at the Gasbuggy and Rulison sites and analytical amplification modeling. Each of these steps is discussed below.

The Gasbuggy BPF data sample was extended from a distance range of 20-90 km to cover a distance range from 4.27 to 90 km by processing close-in strong motion data. Regression equations were scaled to 40 kt and 60 kt using yield extrapolation exponents derived from Nevada Test Site experience.

Recent theoretical studies (Reference 5.2) show that the depth of burial has an effect on the shape of the amplitude-frequency curve. Because Rulson is at a greater scaled depth of burial than Gasbuggy, the PSRV predictions were adjusted accordingly. This technique is based on an extension of Sharpe's problem which describes the effect of an overpressure in a spherical cavity in an infinite, homogeneous, isotropic, and perfectly elastic medium. After scaling for yield and depth of burial, the resulting curves were multiplied by 6.4 to convert from BPF to 5% PSRV spectra. The spectral predictions at Collbran, DeBeque, Silt, Glenwood Springs, Delta, and Montrose (see Figures 2-5 and 2-8) were based on the two steps described above. No refraction data were available at these sites.

Alluvium amplification has been shown to be frequency dependent (Reference 5.3) varying with alluvium thickness and acoustic impedance contrasts between the surface alluvial layers and underlying layers. To determine propagation velocity and layer thickness information, a refraction survey was conducted at each of seven areas of interest in the Rulison area: Grand Valley, Union Carbide Plant, Holmes Mesa, Morrisania Mesa, Harvey Gap Dam, Rifle and Rulison. The refraction survey interpretations are discussed in Appendix A. The physical parameters obtained from these surveys were used as input to a theoretical model to calculate the possible amplification that might result at each site (Appendix B).

As the PSRV predictions for Rulison were extrapolated directly from observed Gasbuggy BPF data, it was necessary to determine if the Gasbuggy data contained some inherent amplification. If such amplification is present, predicted PSRV at Rulison should not be increased by the amplification factor derived from the Rulison refraction surveys, but by some factor less the inherent Gasbuggy amplification. Consequently, six additional refraction surveys were conducted at representative sites at which Gasbuggy motions were recorded. Results of these surveys are also contained in Appendix A. On the basis of the refraction results at these sites and the model studies (Appendix B), it was found that the Gasbuggy data sample does contain an average amplification factor, per unit frequency, of about two. Therefore, one-half of the frequency-dependent amplification factor determined for the seven Rulison locations was applied to the spectral prediction in order to compensate for the amplification inherent in the Gasbuggy data sample.

At Grand Valley, the Union Carbide Plant, and Holmes Mesa, the amplification factors which were applied to the predictions were small (less than a factor of three) relative to the prediction uncertainties.* At Harvey Gap Dam, Rifle, and Rulison, the amplification factors, at frequencies in the range of 7 to 10 Hz, are greater than the uncertainties in the predictions. Amplification factors were not calculated at Morrisania Mesa. However, based on comparisons of refraction survey results, it is assumed that this station would respond in a similar manner as Holmes Mesa. The spectral predictions which include the amplification factors are shown in Figures 2-6, 2-7, 2-9, and 2-10.

*A measure of the uncertainty in the spectral prediction is given in Table 5-1.

5.6 PEAK PARTICLE ACCELERATION NEAR SURFACE ZERO

Peak particle acceleration predictions near surface zero were made after consultation with the Sandia Laboratories and careful analysis of close-in data from two previous nuclear experiments. These were: 1) Gasbuggy, a nuclear experiment to stimulate gas recovery in the San Juan Basin of New Mexico, and 2) Salmon, a nuclear detonation in a salt dome in southern Mississippi. Spall will probably occur near surface zero, and the acceleration level caused by the spall closure signal is estimated to range from 2 - 15 g, with the distinct possibility of higher acceleration values (see Figure 2-11).

TABLE 5-1

UNCERTAINTY ASSOCIATED WITH SPECTRAL PREDICTIONS FOR THE RULISON EVENT

Period	Standard Error of Estimate, σ
2.44	2.35
1.82	2.31
1.33	2.31
1.00	2.42
0.74	2.37
0.54	2.87
0.40	2.61
0.29	2.78
0.22	2.95
0.16	2.95
0.12	3.10
0.09	3.34

Chapter 6

TERMINAL EFFECTS

6.1 ROCK FALLS AND SLOPE STABILITY

A preliminary slope survey was conducted March 3-7, 1969, in conjunction with geologic reconnaissance of the Rulison area. The survey included inspection and evaluation of sites and slopes where failures or rock falls would constitute a hazard to either population centers or rail and highway traffic. Although the general reconnaissance covered the area within 160 km of the proposed Rulison location, a detailed evaluation was conducted within a 30 km radius. Because of poor road conditions, several unimproved roads and jeep trails extending through virtually uninhabited areas within the 30 km radius were not inspected. Examination of geologic and topographic maps of these areas reveal no obvious hazardous situations.

The following areas appeared to be potentially dangerous because of the precipitous nature of the slopes and the common occurrence of natural falls and slides:

1. *DeBeque Pass (30 - 38 km)*—The entire pass is bordered by massive sandstones, underlain by incompetent shales, which are locally exposed. Natural rock falls occur frequently throughout most of the year along both Route 6-24 and the Denver & Rio Grande Railroad. Particularly hazardous is a three hundred yard stretch on the south side of Route 6-24, at the eastern end of the pass. At this point, the road was recently blocked by a fall including one rock mass approximately the size of a car. Considerable evidence exists of other smaller, but hazardous, falls in this area. The appearance of the slope indicates continual recurrence.

2. *One mile east of Silt on Route 6-24 (about 32 km)*— At this spot, a broken, 10-20 foot high sandstone ledge on the north side of the highway appears to threaten a one hundred foot extent of the route. Mass failure appears unlikely. However, as the ledge exists at an inside curve on a hill, thus limiting visibility, even minor falls may indirectly pose a hazard to traffic.

3. *The Route 65-330 Intersection, near Mesa (29 km)*—The site is at a tight corner on the north side of Route 65 about 200 yards west of the intersection. Two car-size masses are poised above the road, but on close examination, both appear relatively stable. The possibility of smaller rocks falling at the turn remains an apparent threat.

4. *Road to Oil Shale Corp. Road, north of Grand Valley (24 km)*—The west side of the recently improved road extending north of the Union Oil Co. plant to the TOSCO (Colony Mine) operation shows signs of recent minor rock falls, and reportedly has undergone serious falls and slides in the past.

5. *Vega Dam Road, east of Collbran (23 km)*—The road is about five miles long extending eastward from the Silt-Collbran road. It is located on the steep northern side of a narrow valley and displays clear evidence of recent major slumping. The entire region, in fact, classically displays continual large scale slumping. The earth fill dam blocks the Plateau Creek Valley, below which lies Collbran. Both the dam and its reservoir appear safely situated in regard to slumping.

6. *Plateau Creek Canyon 30 - 38 km)*—The western half of Route 65-330 which extends from Collbran to Route 6-24, passes through a narrow, steep-walled canyon composed chiefly of massive sandstone, equivalent to those of those of DeBeque Canyon. Although the rock appears generally competent, overhangs of fractured material, and evidence of recent rockfalls are numerous.

7. *Glenwood Canyon (57 - 75 km)*—Immediately east of Glenwood Springs, both Route 6-24 and the Denver and Rio Grande Railroad pass through the narrow, steep-sided canyon of the Colorado River. Rockfalls, both on the road and railroad occur frequently throughout most of the year.

Because of the frequency of naturally occuring rockfalls in the above areas, it is expected that rail and highway traffic near the above locations will be subjected to rockfall hazards at shot time.

Peak resultant particle acceleration, scaled from the Gasbuggy data, at distances corresponding to the locations mentioned above are given in Table 2-5.

6.2 SEISMIC HAZARDS TO UNDERGROUND STRUCTURES

The only underground facilities within the vicinity are three oil shale mines north of the test site. These are the Mobil Oil and U.S. Bureau of Mines facility at Anvil Points (14.5 km); the Union Oil Company of California workings (~ 23 km), and the TOSCO facility (Colony Mine) (~ 25 km). From Figure 2-4, the predicted resultant vector surface motions for the maximum yield at these sites are 0.2g, 0.06g, and <0.06g, respectively.

Thresholds of seismic damage to subsurface structures presumably depend upon many parameters, and they are not well understood. Reference 6.1 suggests that surface accelerations of 0.4 to 0.8 g's may represent minimum values at which damage may occur. Using these criteria, none of the three sites mentioned above should suffer damage. However, because of the uncertainties involved in these criteria and the relatively large dimensions of the underground working, rockfalls and other minor damage appear possible at Anvil Points. The other two mines are sufficiently close that rockfalls are a possibility.

6.3 POSSIBLE EFFECTS ON STREAM FLOW FROM SPALLING AND BANK FAILURE

As stated in Chapter 4, surface spalling will be negligible and should affect only the unconsolidated surface materials. Vertical fracturing will probably be minor and should not significantly affect the regimen of the East Fork of Battlement Creek, passing about 250' southwest of surface ground zero.

The combination of a relatively steep local topographic gradient, presence of local springs and ponds, and the perennial nature of local streams indicates a shallow water table within the unconsolidated surface sediments near ground zero. It appears, therefore, that surface fracturing will neither increase downward percolation of stream waters nor create more than a temporary, minor disturbance to the stream's flow or overall regimen.

Because of the small amount of anticipated spalling, resultant permanent displacements are not expected to be sufficient to cause stream blockage. However, partial blockage from bank collapse appears probable, particularly along the 30 - 40 ft. bank adjacent to the G.Z. fill. The stream flow effects of such partial blockage appear inconsequential. As with damming from naturally occurring bank collapse, minor ponding would probably occur and continue until the rising water topped the lowest portion of the barrier, at which time the unconsolidated slump materials would be rapidly breached and distributed downstream. Even in the unlikely event of substantial blockage, a resultant water surge at the time of breaching would be substantially dissipated before reaching populated areas downstream. Except for temporary ponding, stream regimens would remain unaffected.

REFERENCES

2.1 Rulison Project Definition Plan; December 9, 1968.

3.1 Tentative Operational Plan–Project Rulison (Rough Draft); November 27, 1967.

3.2 Yeend, Warren E.; "Quaternary Geology of the Grand-Battlement Mesa Area, Colorado;" USGS Reports–Open File Series; No. 945; October 30, 1967.

3.3 Voegeli, Paul T., Sr.; "Geology and Hydrology of the Project Rulison Exploratory Hole, Garfield County, Colorado;" USGS Open File Report–474-16, Rulison-1; April 4, 1969.

4.1 Environmental Research Corporation; "Summary Report of Predictions, Gasbuggy Event;" NVO-1163-124; Alexandria, Virginia; November 1, 1967.

4.2 Rawson, D. E., J. A. Korven, R. L. Pritchard, and W. Martin; "Gasbuggy Post-Shot Geologic Investigations;" PNE-G-11; Lawrence Radiation Laboratory, Livermore, California; November 1968.

4.3 Essoglou, M. E. and D. G. Rogich; "A Simplified Method for Predicting Free-Field Displacements and Strains;" NVO-1163-43; Roland F. Beers, Inc.; Alexandria, Virginia; December 1964.

4.4 Roland F. Beers, Inc.; "Analysis of Shoal Data on Ground Motion and Containment;" VUF-1013 (NVO-1163-30); Alexandria, Virginia; December 1964.

5.1 Lahoud, J. A. and J. R. Murphy; "Analysis of Seismic Peak Amplitudes from Underground Nuclear Explosions;" Bull. Seismol. Soc. Am.; in press, Dec., 1969.

5.2 Mueller, R. A.; "Seismic Spectrum Scaling Law;" (Abstract); *Transactions of the American Geophysical Union*; Vol. 50, No. 4, pg. 248; 1969.

5.3 Davis, A. H. and J. R. Murphy; "Amplification of Seismic Body Waves by Low-Velocity Surface Layers;" NVO-1163-130; Environmental Research Corporation; Alexandria, Virginia; December 1967.

6.1 Letter: ERC-11209 by S. B. Smith; Earthquake Hazards to Chamber Construction, Amchitka; December 4, 1967.

APPENDIX A
REFRACTION SURVEYS

PURPOSE

Many locations in the Rulison area are covered with relatively thin alluvial layers which can sometimes cause ground motions to be amplified (Reference 5.3). The amount of amplification and the frequency at which it occurs depend on the thickness of the surface layers and the acoustic impedance contrast between the surface layers and underlying layers.

Refraction surveys were conducted at seven locations to determine the thickness of the surface layer and the propagation velocities of the surface layer and underlying layers. Reverse profile refraction data were collected at Rifle, Rulison, Grand Valley, Holmes Mesa, Morrisania Mesa, the Union Carbide Plant and Harvey Gap Dam. Using standard refraction techniques, the data were analyzed and interpreted. A diagrammatic illustration of a refraction array, the seismic energy travel paths, and the graphical determination of layer velocities are shown in Figure A-1.

In addition to the surveys conducted in the Rulison area, several were made in locations in northwestern New Mexico that were instrument stations for the Gasbuggy event. These included two hard rock-alluvium pairs—Blanco (Station 23) and Farmington (Station 31), and four alluvium stations—Bloomfield (Station 28), Dulce (Stations 15 and 16), La Jara Ranch (Station 9), and the Dzilth-Na-O-Dith-Hle School (Station 26). These stations allow a direct comparison of refraction survey data with recorded Gasbuggy motions and give a measure of the amplification inherent in the Gasbuggy data. Results of the Rulison surveys are shown in Figures A-2 through A-4; the Gasbuggy survey results in Figures A-5 and A-6.

ERROR ANALYSIS

The errors associated with the determination of seismic velocities and the depth to an interface from the field data may be calculated by methods discussed in Reference A-1. Briefly, if A, B, and C are measured values of physical phenomena, and if

$$K = A \cdot B \cdot C$$

then the probable error in K, δK, is given by

$$(\delta K)^2 = \left[\frac{\partial K}{\partial A}\ \delta A\right]^2 + \left[\frac{\partial K}{\partial B}\ \delta B\right]^2 + \left[\frac{\partial K}{\partial C}\ \delta C\right]^2$$

where δA, δB, δC are the maximum errors in the measurements.

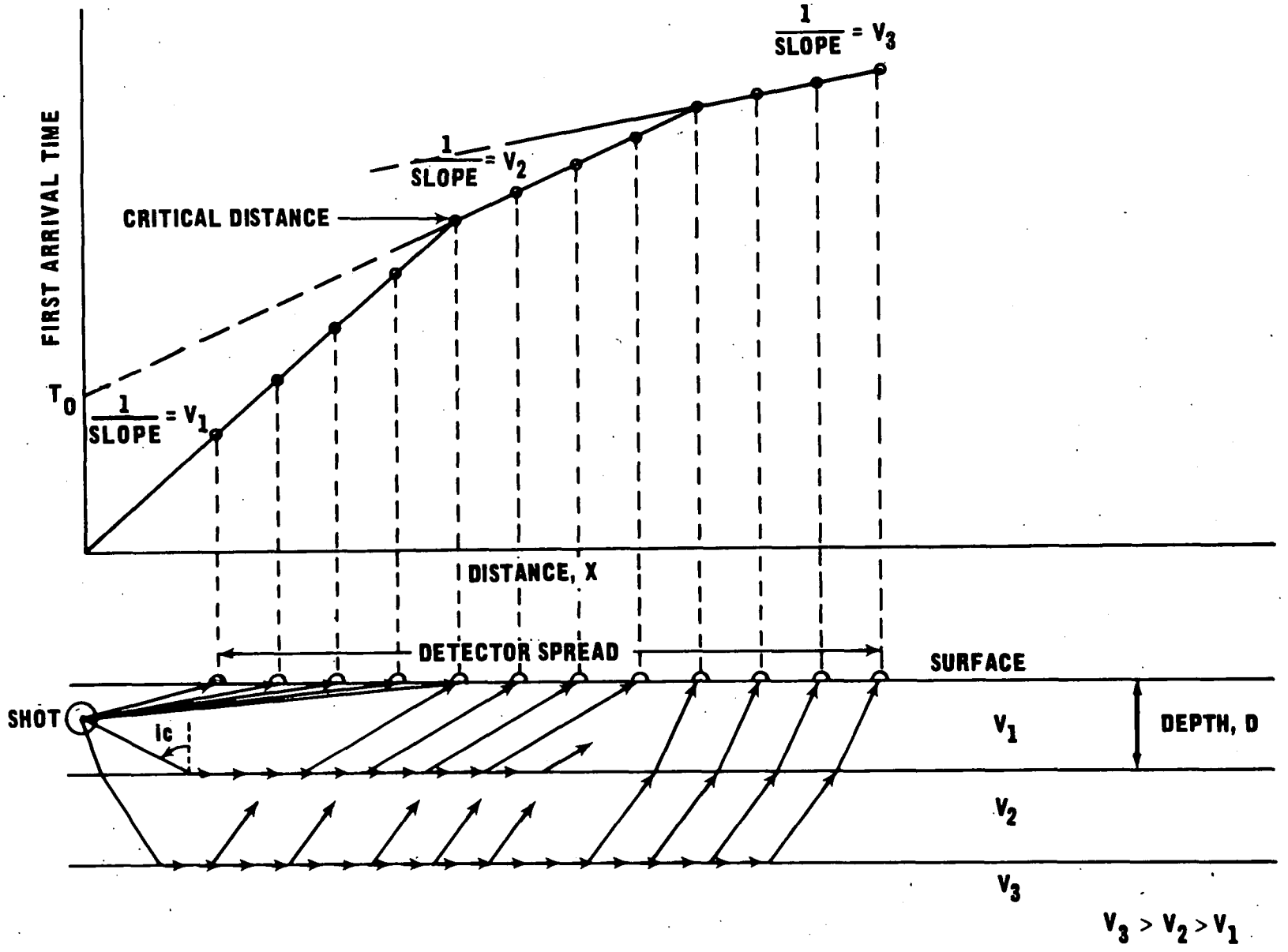

Figure A-1. Schematic Representation of the Elements Involved in a Seismic Refraction Survey

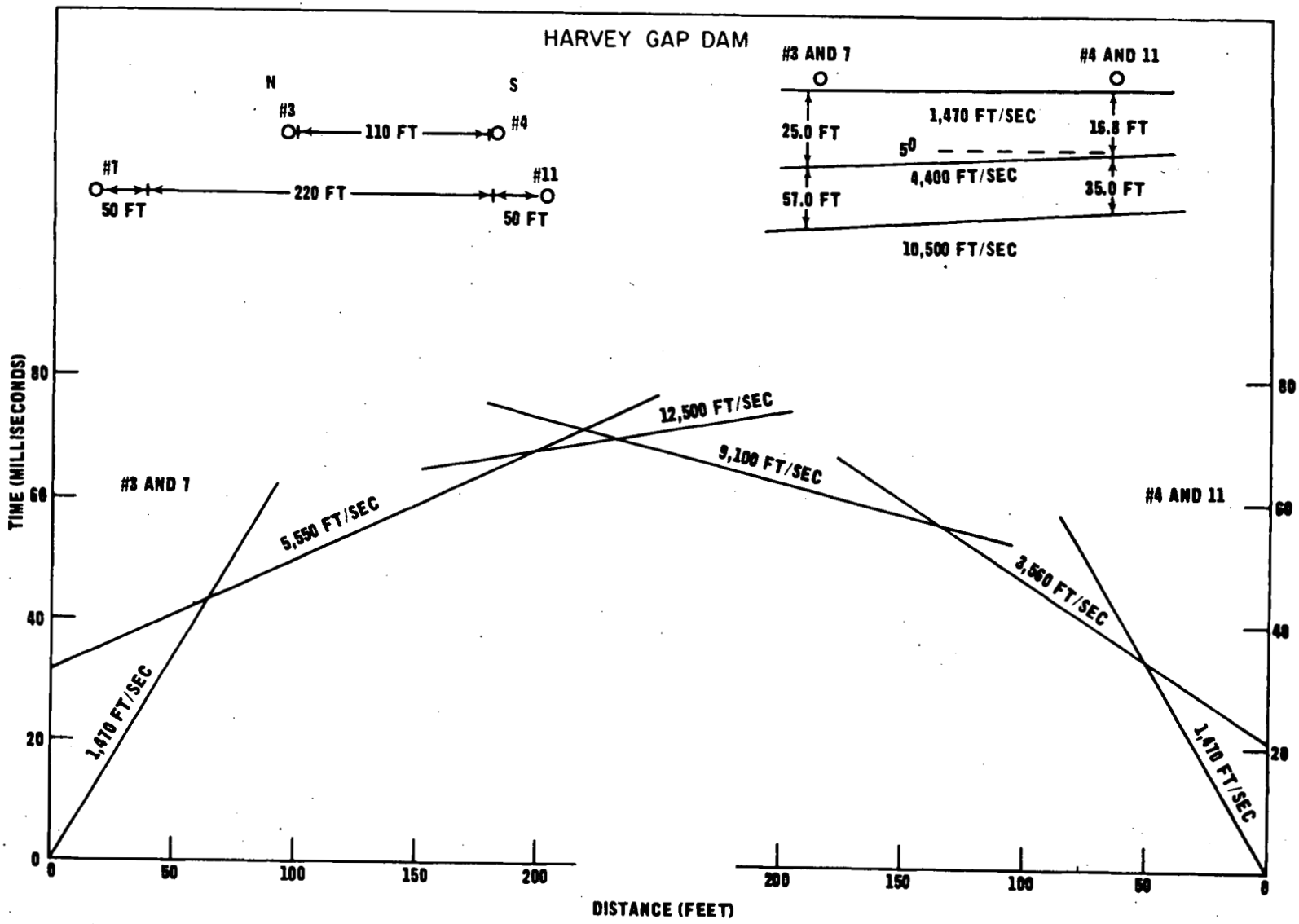

Figure A-2. Interpretation of Refraction Survey Data

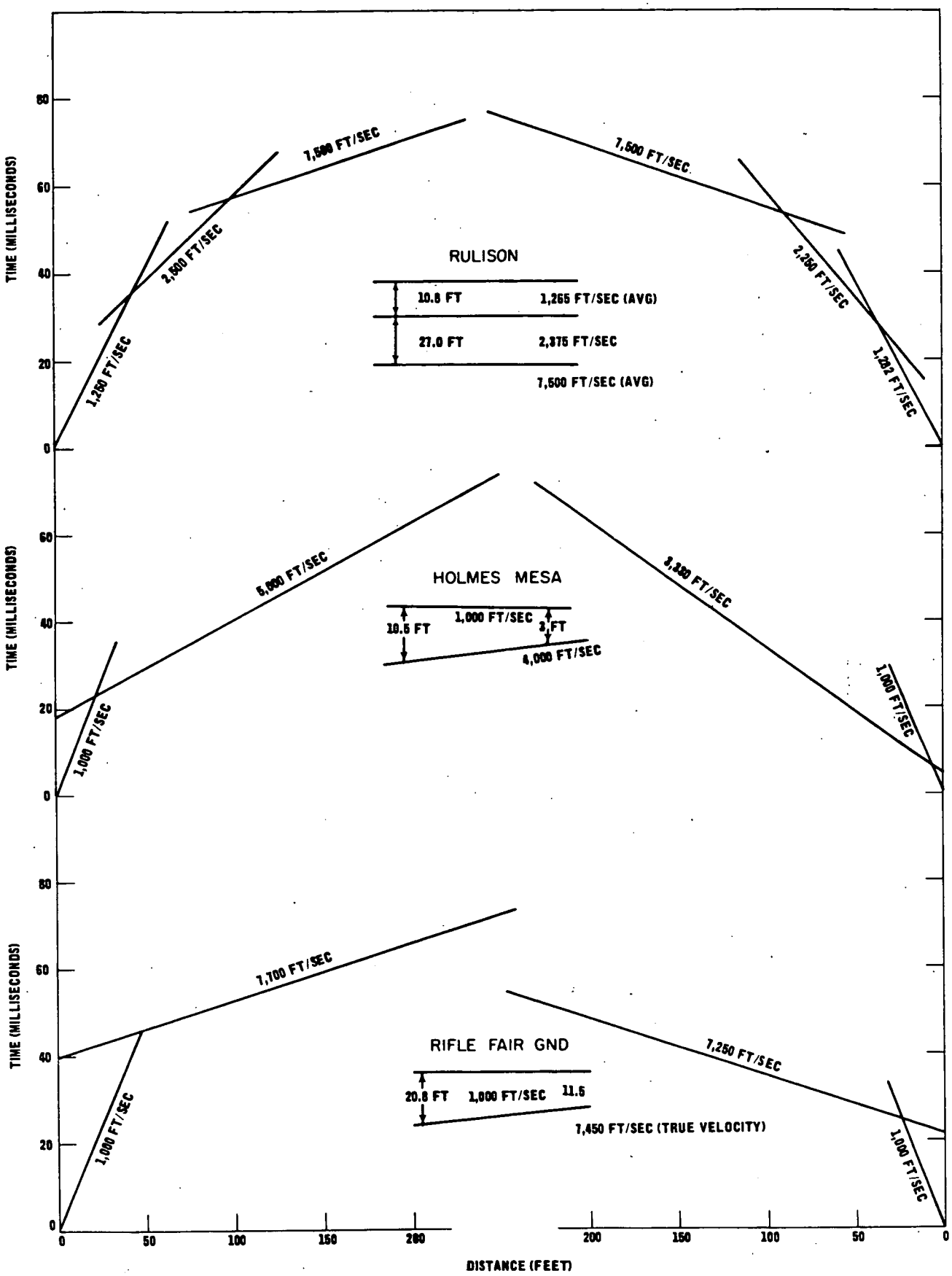

Figure A-3. Interpretation of Refraction Survey Data

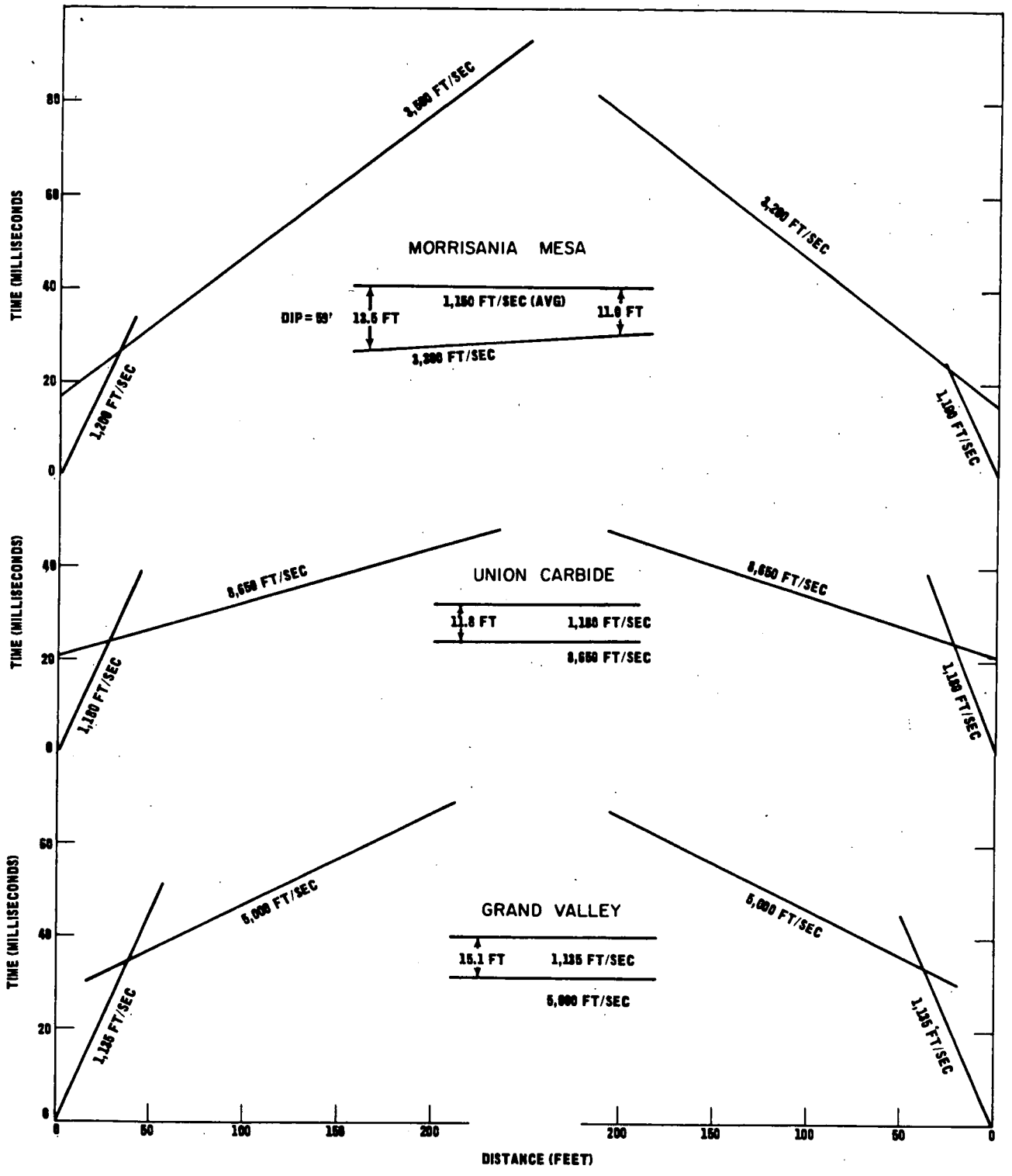

Figure A-4. Interpretation of Refraction Survey Data

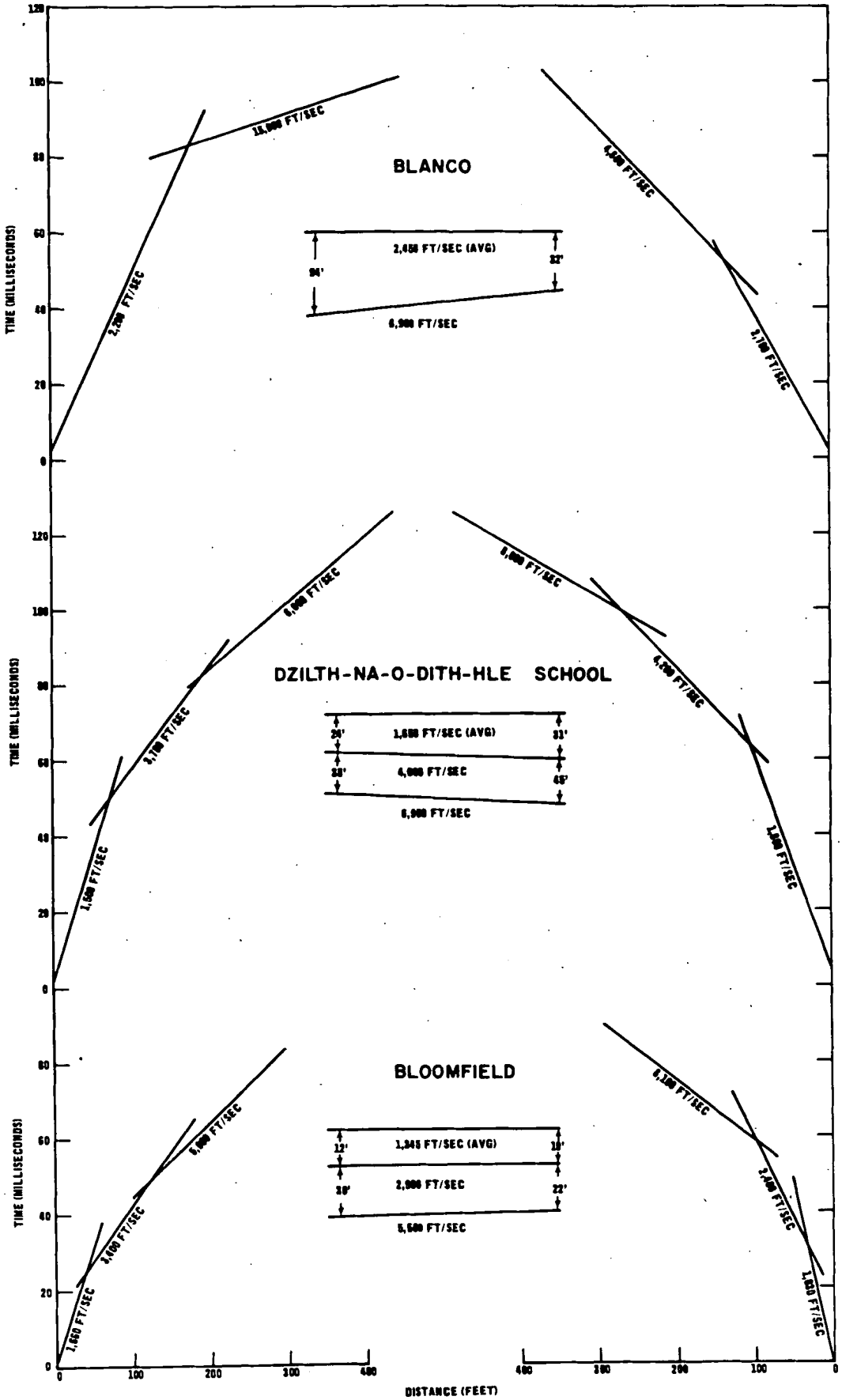

Figure A-5. Interpretation of Refraction Survey Data

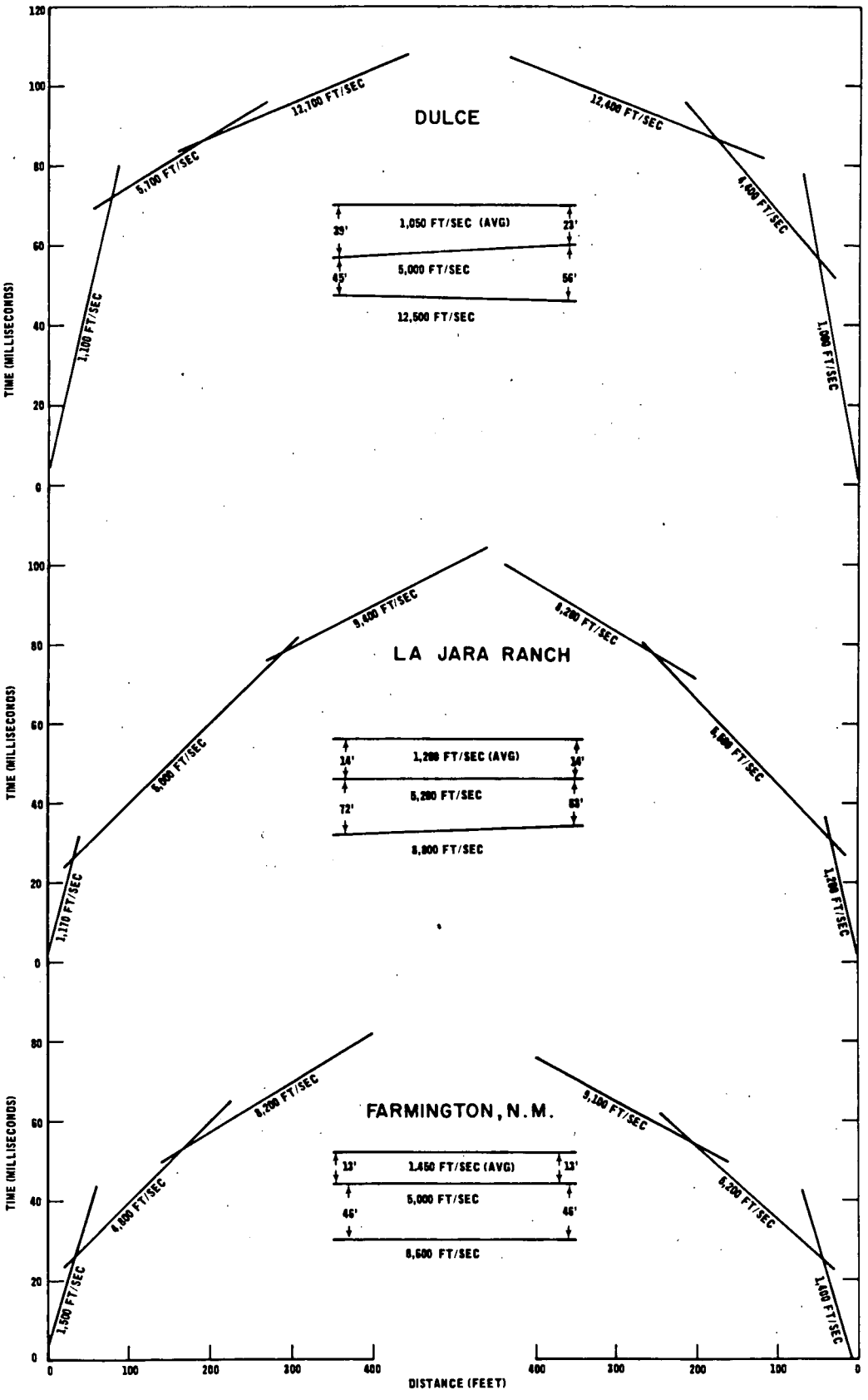

Figure A-6. Interpretation of Refraction Survey Data

Referring to Figure A-1, the values of velocity, critical distance, and depth to an interface are given by

(1) $V = X/T$

(2) $$X_c = \frac{T_0 V_1 V_2}{V_1 - V_0}$$

(3) $$D = \frac{X_c}{2} \sqrt{\frac{V_1 - V_0}{V_1 + V_0}}$$

where

V = Velocity
X = Distance
X_c = Critical Distance
T = Time
D = Depth
T_0 = Time intercept at X = 0
V_0 = Velocity of surface layer
V_1 = Velocity of underlying layer

The probable errors in velocity, critical distance, and depth are, from equations (1), (2), and (3), respectively

(4) $$[\delta V]^2 = \left[\frac{1}{T}\ \delta X\right]^2 + \left[-\frac{X}{T^2}\ \delta T\right]^2$$

(5) $$[\delta X_c]^2 = \left\{\frac{T_0 V_1}{V_1 - V_0}\left[1 + \frac{V_0}{(V_1 - V_0)}\right]\delta V_0\right\}^2 \quad \text{for } \frac{\partial X_c}{\partial T_o} = 0$$

$$+\left\{\frac{T_0 V_0}{V_1 - V_0}\left[1 - \frac{V_1}{(V_1 - V_0)}\right]\delta V_1\right\}^2 \quad \text{for } \frac{\partial X_c}{\partial T_o} = 0$$

(6) $$[\delta D]^2 = \left\{\frac{1}{2}\sqrt{\frac{V_1 - V_0}{V_1 + V_0}}\ \delta X_c\right\}^2 + \left\{\frac{X_c}{4}\sqrt{\frac{V_1 + V_0}{V_1 - V_0}}\ \delta V^1\right\}^2$$

where

$$V^1 = \sqrt{\frac{V_1 - V_0}{V_1 + V_0}}$$

Data from five profiles in the vicinity of the Harvey Gap Dam were used to calculate errors in seismic velocity determination and the depth to underlying layers. The results are given in Table A-1.

TABLE A-1
ERRORS ASSOCIATED WITH HARVEY GAP DAM REFRACTION SURVEY

Shot Line	Instrumental Error in Velocity (%)	Average Error in Fitting Lines to Velocity Data (%)	Total Error in Velocity (%)	Instrumental Error in Depth (%)	Total Error in Depth[1] (%)
3-4	1.9	2.8	3.4	4.6	7.6
15-6	1.8	3.2	3.7	3.1	8.2
9-13	0.7	3.4	3.5	2.9	8.6
8-12	1.3	1.7	2.2	3.9	6.1
16-17	1.9	6.9	7.9	6.2	25

[1]Includes the effect of the error in the critical distance.

INTERPRETATION OF RESULTS

The results and interpretation of the refraction data collected at the seven Rulison locations are given in Figures A-2 through A-4. At Morrisania Mesa, the Union Carbide Plant, Grand Valley, Holmes Mesa and Rifle (Fairgrounds) the surface layer was found to be between 3 and 20 feet thick and to have a compressional velocity of 1000 to 1180 ft/sec depending on the particular location. The velocity of the underlying layer varied from 3300 ft/sec at Morrisania Mesa to 8650 ft/sec at the Union Carbide Plant. At Rulison and Harvey Gap Dam, the interpretations show a low velocity surface layer, an intermediate velocity layer, and a deeper high velocity layer. These interpretations are consistent with the results of geologic investigations conducted by John A. Blume & Associates and ERC at these locations.

Results obtained from the refraction survey at each of six selected Gasbuggy sites (Figures A-5 and A-6) show that the surface layers have compressional velocities and thicknesses comparable to those at Rulison. The surface layer varied between 10 and 94 feet in thickness and the velocities varied between 1050 and 2450 ft/sec. An intermediate layer, ranging in thickness from 22 to 72 feet and in velocity from 2900 to 5200 ft/sec, overlies the deeper high velocity (5500 to 12,500 ft/sec) layer.

The results of the refraction surveys at Rulison and Gasbuggy were used to evaluate the possibility of amplification of ground motion due to the presence of the low velocity surface layers. This procedure is described in Appendix B.

REFERENCES

A-1. Topping, J.; (1956); *Errors of Observation and Their Treatment*; Institute of Physics, pg. 119.

Appendix B
STATION FACTOR CALCULATIONS

In Appendix A the unit thicknesses and compressional velocities derived from seismic refraction surveys at locations of interest with regard to the Rulison experiment have been presented. These data provide an input to the seismic amplification models used for station factor calculations.

Although operational mathematical models are currently available to describe the amplification of both body (P, SV, SH) and surface (Love, Rayleigh) waves (References B-1, B-2, B-3) the present study concentrated on body waves because of the relative thinness of the layers involved and the proximity of the stations to the shot point. The body wave models are based on the Haskell matrix formulation (Reference B-4) for the transmission of plane body waves through a sequence of plane parallel, perfectly elastic layers. The problem in this formulation is linear. Consequently, the Fourier amplitude spectrum of the output at the earth's surface can be related to the Fourier amplitude spectrum of the input wave at the base of the layered sequence by a transfer function. This function characterizes the effect of the layered sequence on the resulting spectral composition. In general, the response depends on (1) the input wave type (P, SV, SH), (2) the angle of incidence of the input plane wave, and (3) the elastic parameters (compressional and shear velocities, density) and thicknesses of the various layers. Some insight is provided by considering the most simple case; that of a single layer overlying a halfspace subjected to a normally incident wave. In this case, the lowest frequency at which maximum amplification will occur is given by $c/4h$ where c is the propagation velocity of the wave of interest (P, SV, SH) in the layer and h is the layer thickness. This is analogous to the familiar quarter-wavelength condition used in the study of electromagnetic and acoustic waves. In this case, the amplitude of the maximum amplification is given by $c_2\rho_2/c_1\rho_1$ where ρ is the density and the subscript 1 denotes the layer while the subscript 2 denotes the halfspace.

In computing the theoretical response at the Rulison sites of interest, a combination of the refraction survey data presented in Appendix A together with judgment based on prior experience at the Nevada Test Site (NTS) was used to arrive at physical properties, layer thicknesses and angles of incidence. The compressional wave velocities were determined directly from the refraction data, subject to the qualifications on accuracy noted in Appendix A. The shear wave velocity was then taken to be six-tenths of the compressional wave velocity in accordance with customary procedure (Reference B-5). The densities and angles of incidence were chosen on the basis of NTS experience.

The calculated amplification factors for the six Rulison sites are shown in Figures B-1 through B-6 for incident P and incident SV waves. The geological models employed are shown on each figure. In these figures, the curves correspond to the horizontal amplification factor which is of interest with regard to structural response. It can be seen from these figures that substantial amplification occurs for some of the models.

In order to apply the above curves to the prediction of modified amplitude-frequency content, some judgment based on past experience must be employed. First, experience at verifying the mathematical models at NTS has shown that high frequency peaks (>10 Hz) are usually greatly diminished due to departures from perfect elasticity in the near surface layers. For this reason, amplification above 10 Hz is not considered for prediction purposes. Another factor to be considered is that the amplification curves correspond to ratios of the calculated Fourier amplitude spectra. That is, they correspond, in the frequency domain, to the response of the layered system to an isolated input wave. Consequently, these factors cannot be associated with the amplitude of a given arrival in the time domain (e.g., the peak amplitude). Furthermore, since the anticipated seismogram consists of many arrivals of different wave types with different angles of incidence, the application of these amplification factors, even to a frequency dependent amplitude prediction (i.e., the PSRV curve) is not straightforward. However, experience with NTS data has indicated that the PSRV amplitudes are amplified in a frequency dependent manner which correlates reasonably well with amplifications predicted on the basis of the mathematical model.

In the present case, the amplitude-frequency predictions have been made on the basis of equations statistically derived from the Gasbuggy data (cf. Chapter 5 of this report). The question then arises as to whether the predicted PSRV curves correspond to the basic hard rock situation, or whether some amplification is already implicit in the prediction equations due to the fact that hard rock and alluvium station data were grouped together in deriving the Gasbuggy equations. In an attempt to answer this question, refraction surveys were conducted at six representative Gasbuggy alluvium stations. The results and interpretation of this survey are shown in Appendix A. As with the Rulison refraction data, the derived geological models at Gasbuggy were used as input to the body wave amplification programs. The resulting amplification curves are shown in Figures B-7 through B-12. Two of these sites (Blanco and Farmington) consisted of pairs of stations (hard rock and alluvium) which recorded the Gasbuggy event. The observed BPF ratios at these stations (alluvium/hard rock) are shown in Figure B-13 (solid line) together with the theoretical amplification calculated on the basis of the refraction results (dashed line). It can be seen that the calculated amplification is in good agreement with the observed with regard to amplitude but that the frequency at which the peak amplification occurs at Blanco is somewhat different. Since the velocities and depths determined from refraction surveys can vary within 20%, the theoretical amplification was recalculated using modified values for these parameters. The results of this calculation are shown as a dotted line on Figure B-13, indicating the sensitivity of the model to uncertainties in the elastic parameters. Thus, the amplification model seems to be in reasonably good agreement with the observed data.

On the basis of these observations, it is clear that some amplification is implicit in the Gasbuggy prediction equations. In an attempt to obtain an average Gasbuggy amplification factor, the following reasoning was employed. First, it is noted (cf. Figures B-7 through B-12) that no amplification is observed below 3 Hz. Further, above 3 Hz substantial amplification occurs, the frequency and magnitude of which are subject to the uncertainties in the measured elastic parameters. Since some of the peaks are quite narrow, a direct average as a function of frequency was deemed inadvisable. Rather, it was decided to determine a frequency independent amplification factor (between 3 and 10 Hz) by estimating the average amplification per unit cycle. This was carried out by calculating the area under the amplification curves (using the incident P or SV curve, depending on which gave the maximum amplification) and redistributing this area uniformly under a rectangle extending from 3 to 10 Hz. The height of this rectangle was calculated to be 3.2 units; i.e., the average amplification factor for the alluvium stations is 3.2. Eleven of the Gasbuggy stations used in the derivation of the prediction equations were situated on hard rock while thirteen were situated on alluvium. Considering the amplification factor for the hard rock stations to be unity leads to the results that on the average, the Gasbuggy equations contain an implicit amplification factor above hard rock, of 2.2. Consequently, the peak amplifications calculated for the Rulison sites were reduced by a factor of two before applying them to the predictions made on the basis of the Gasbuggy equations. The implementation of this correction scheme is described in Chapter 5 of this report.

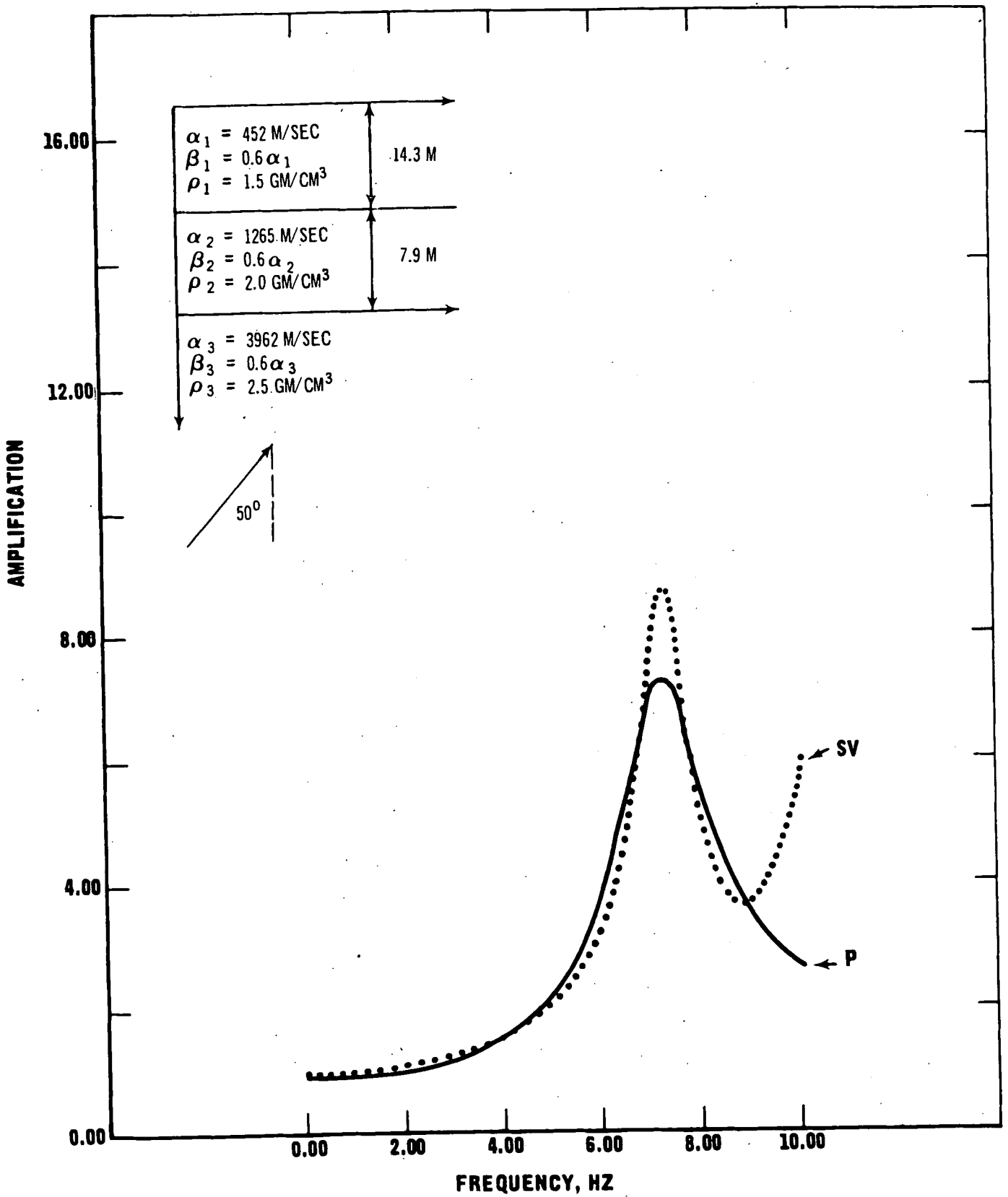

Figure B-1. Horizontal Amplification versus Frequency, Harvey Gap Dam

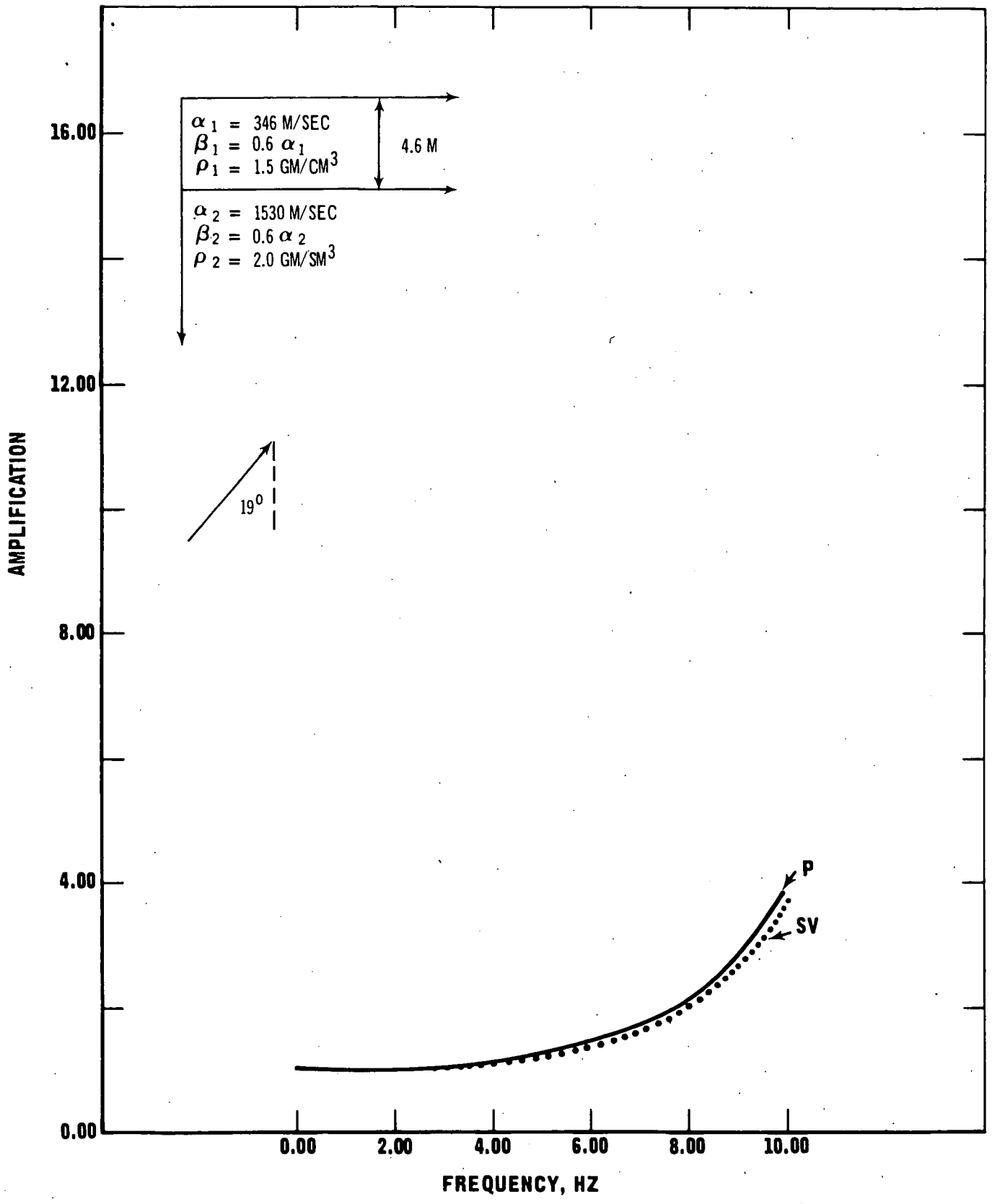

Figure B-2. Horizontal Amplification versus Frequency, Grand Valley

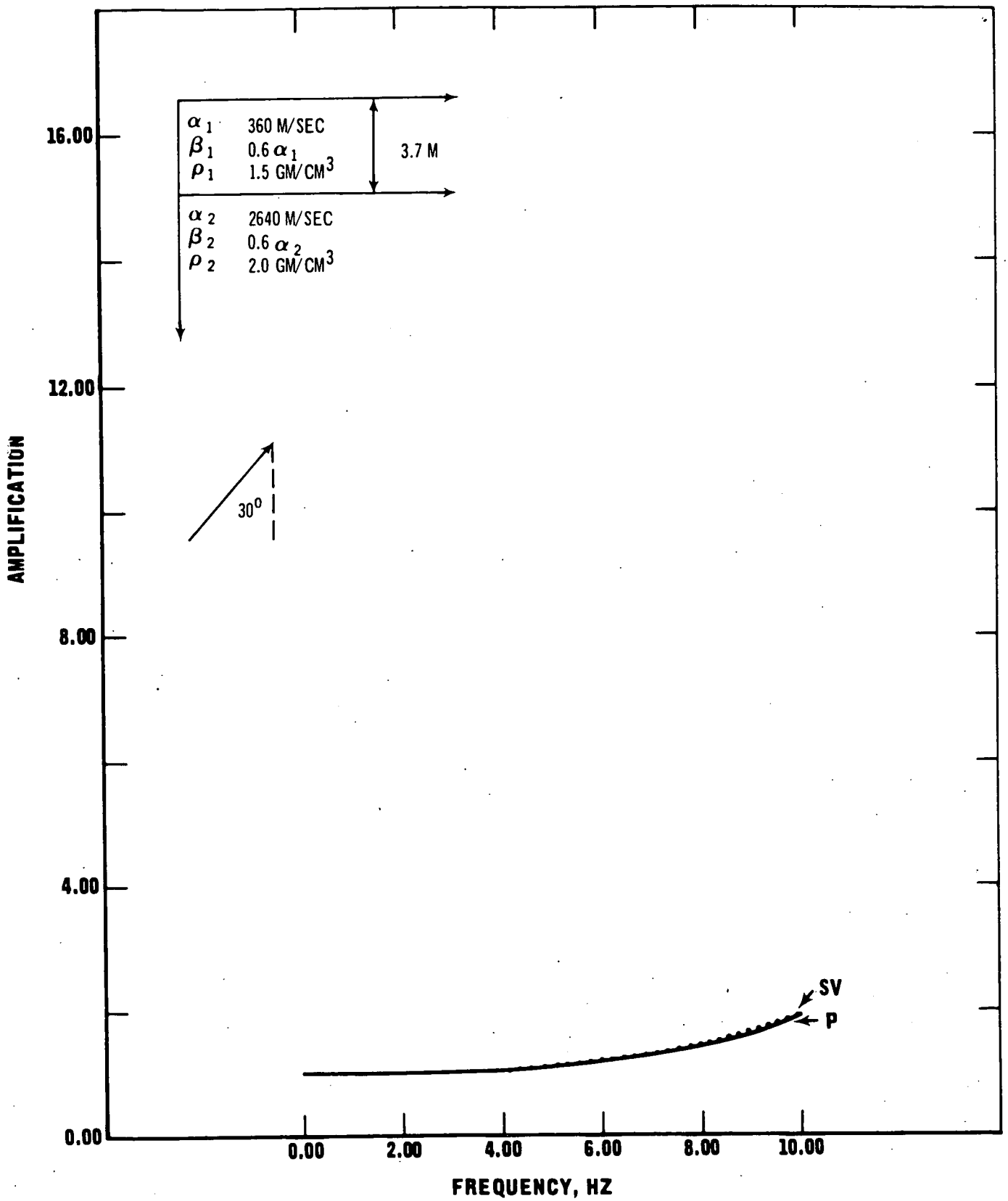

Figure B-3. Horizontal Amplification versus Frequency, Union Carbide

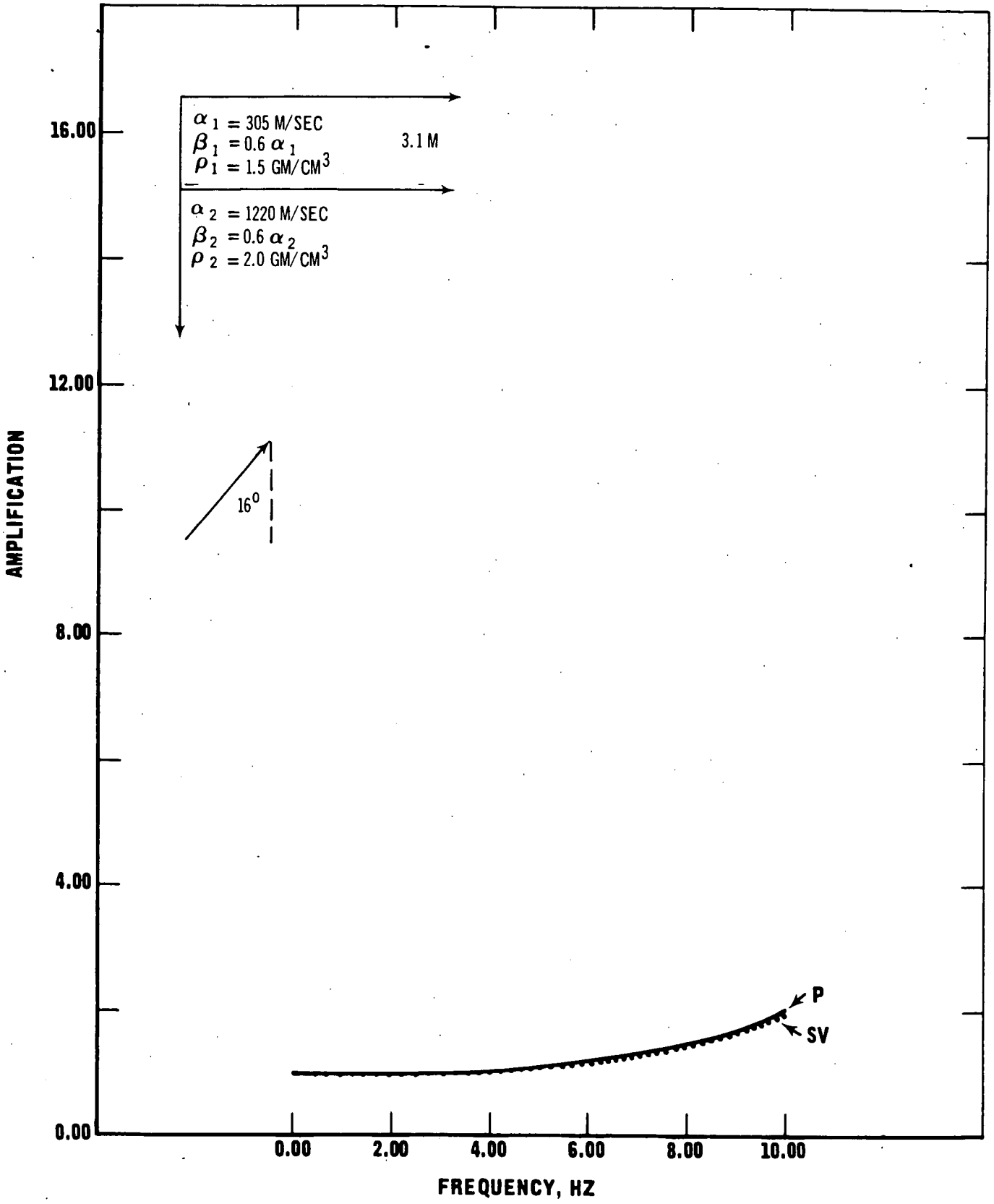

Figure B-4. Horizontal Amplification versus Frequency, Holmes Mesa

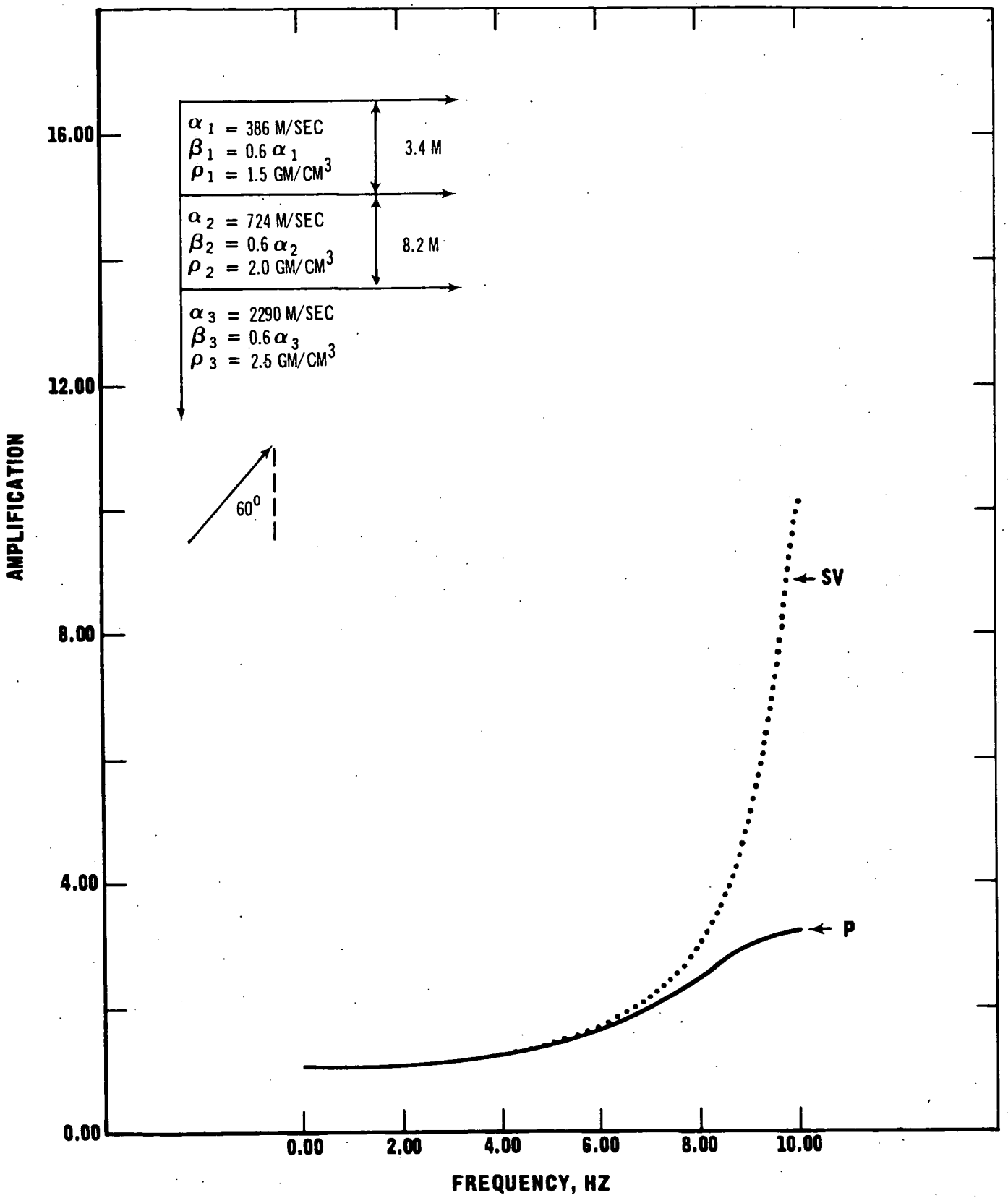

Figure B-5. Horizontal Amplification versus Frequency, Rulison

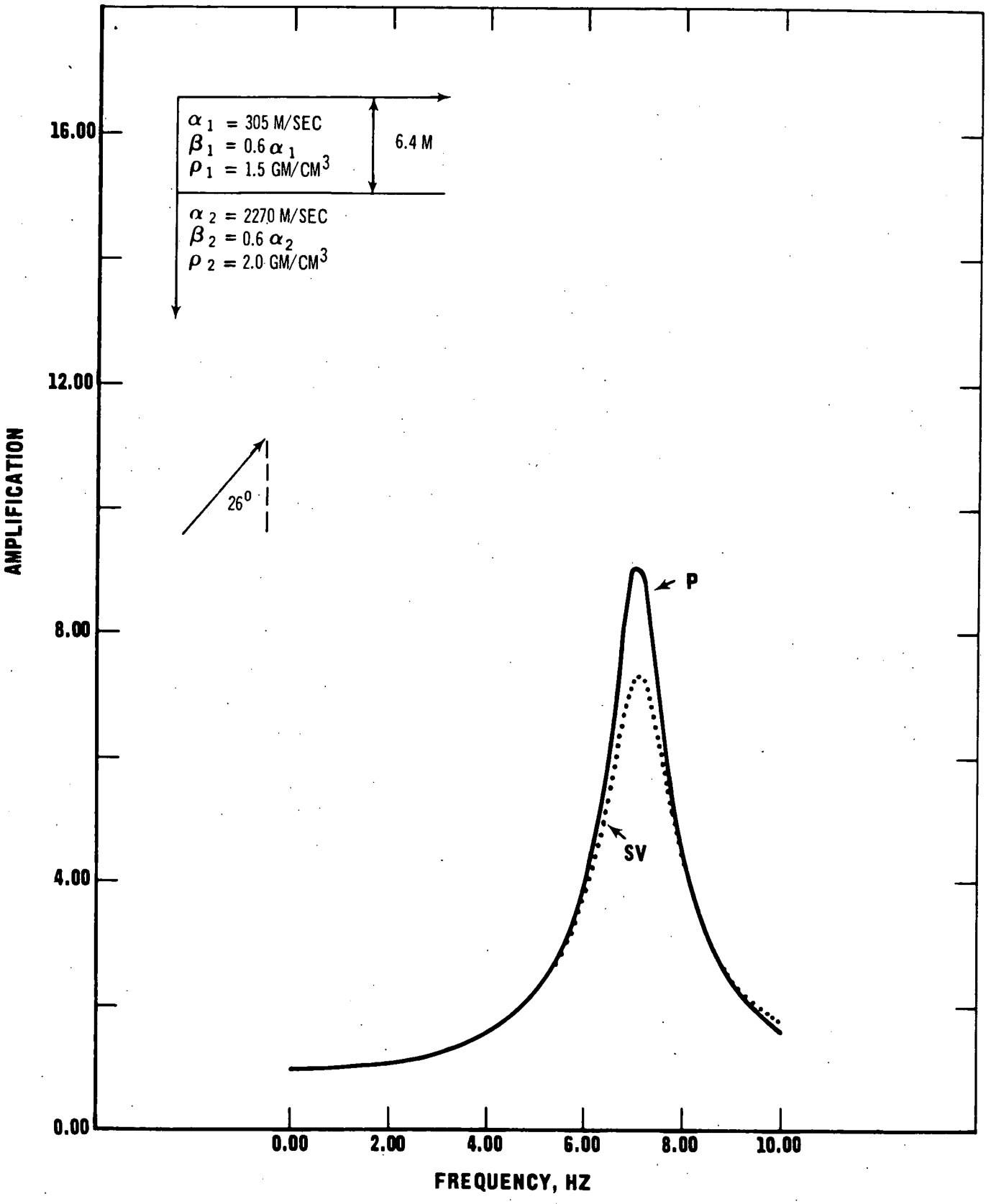

Figure B-6. Horizontal Amplification versus Frequency, Rifle

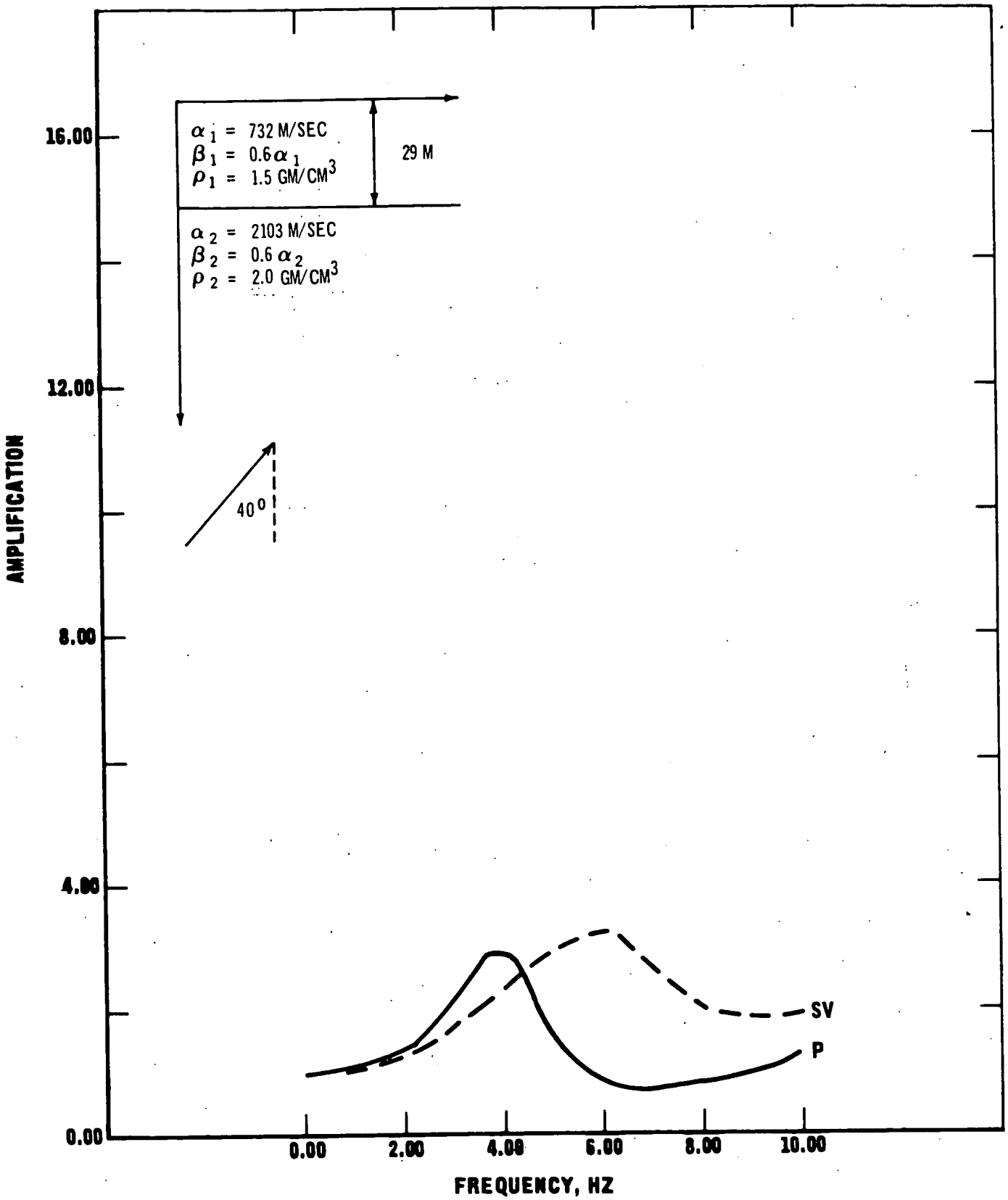

Figure B-7. Horizontal Amplification versus Frequency, Blanco

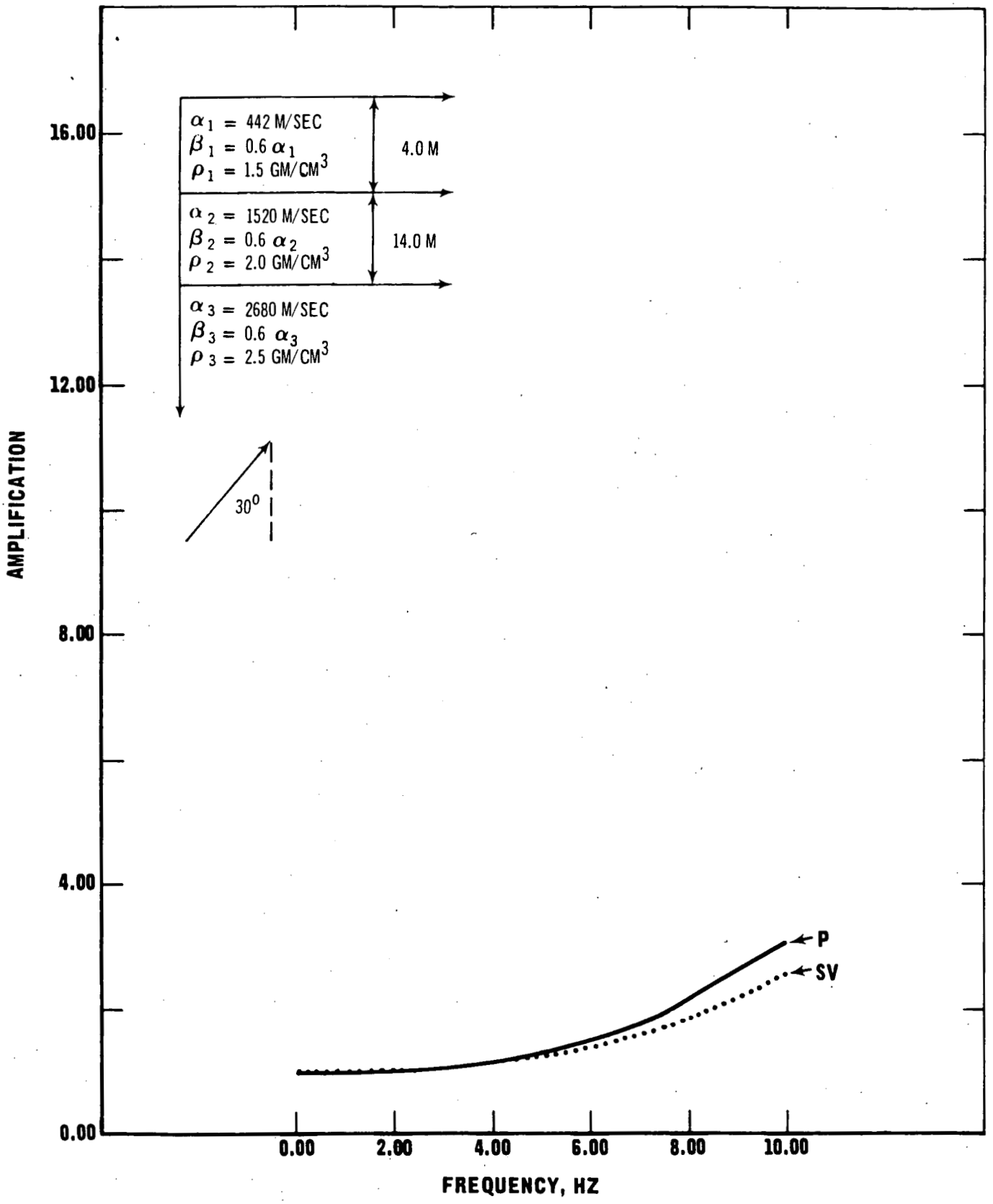

Figure B-8. Horizontal Amplification versus Frequency, Farmington

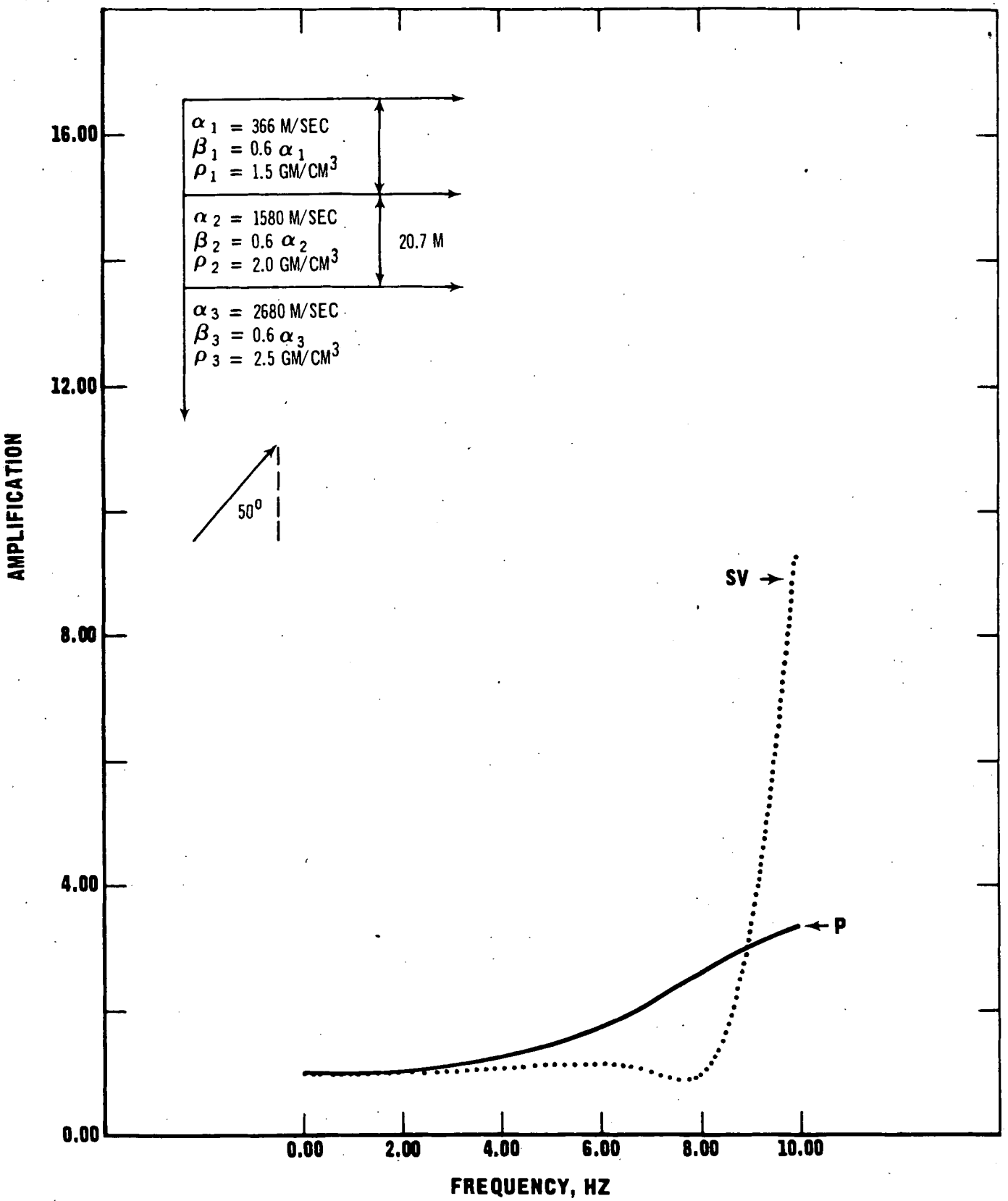

Figure B-9. Horizontal Amplification versus Frequency, La Jara

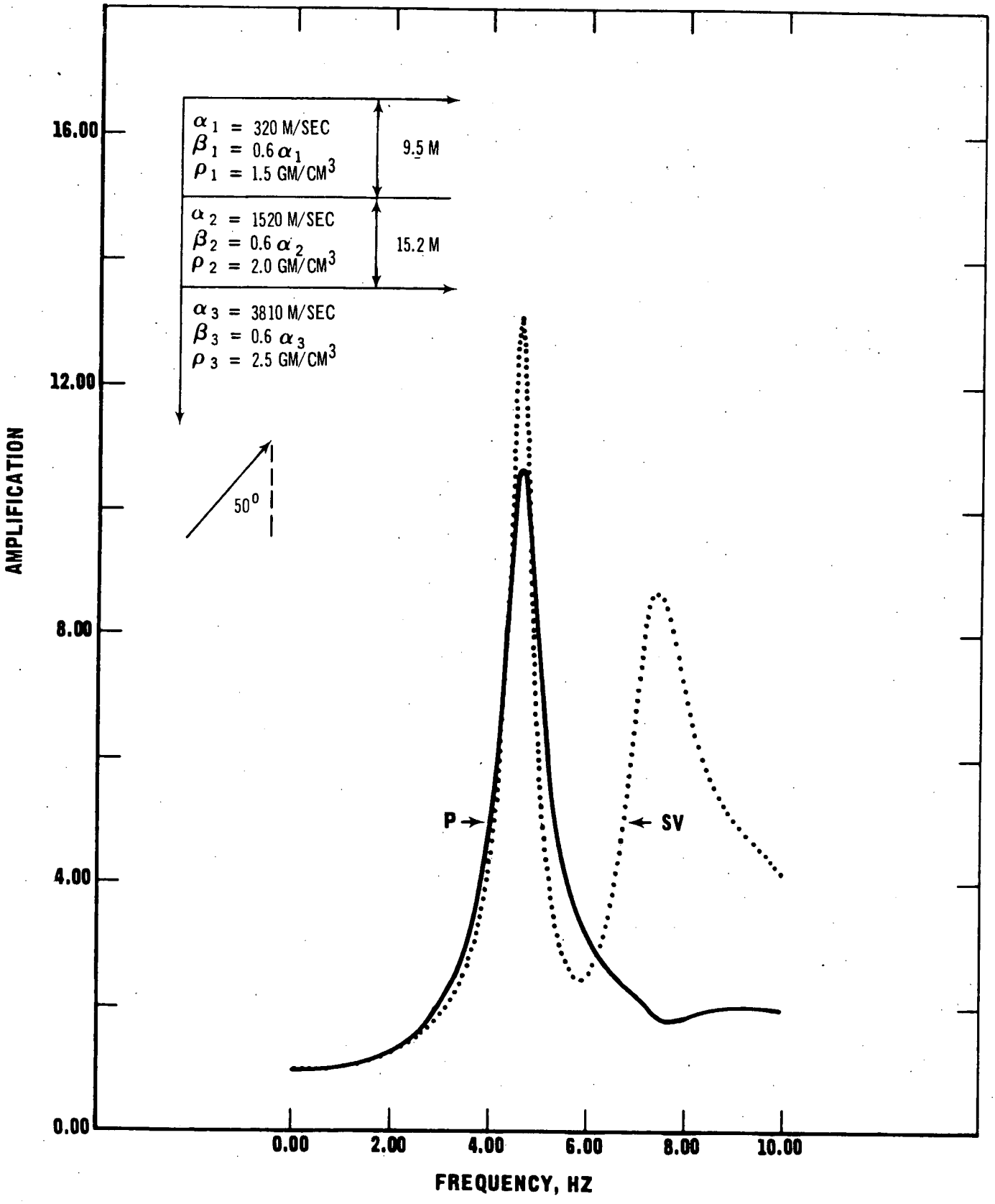

Figure B-10. Horizontal Amplification versus Frequency, Dulce

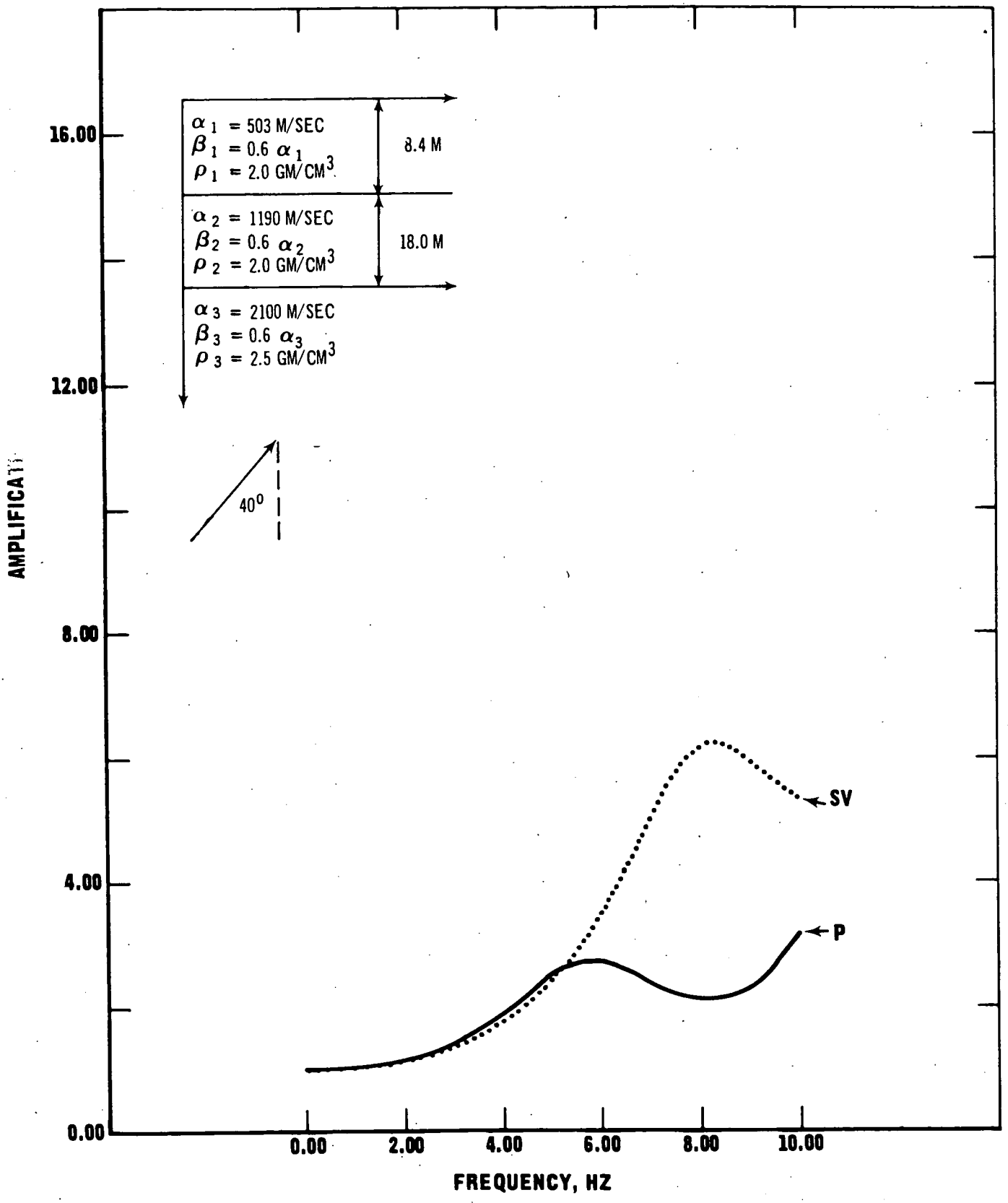

Figure B-11. Horizontal Amplification versus Frequency, Dzilth-Na-O-Dith-Hle School.

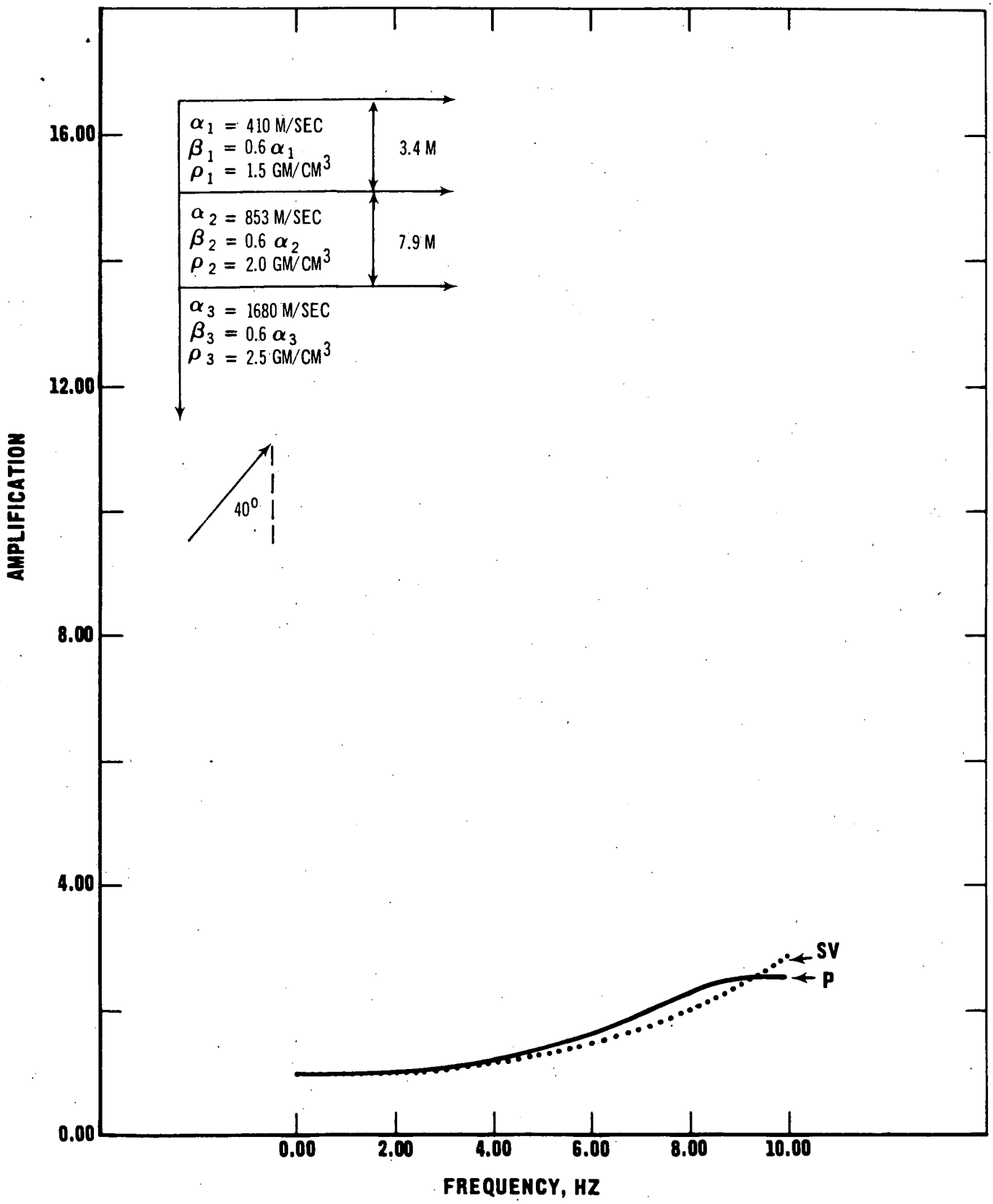

Figure B-12. Horizontal Amplification versus Frequency, Bloomfield.

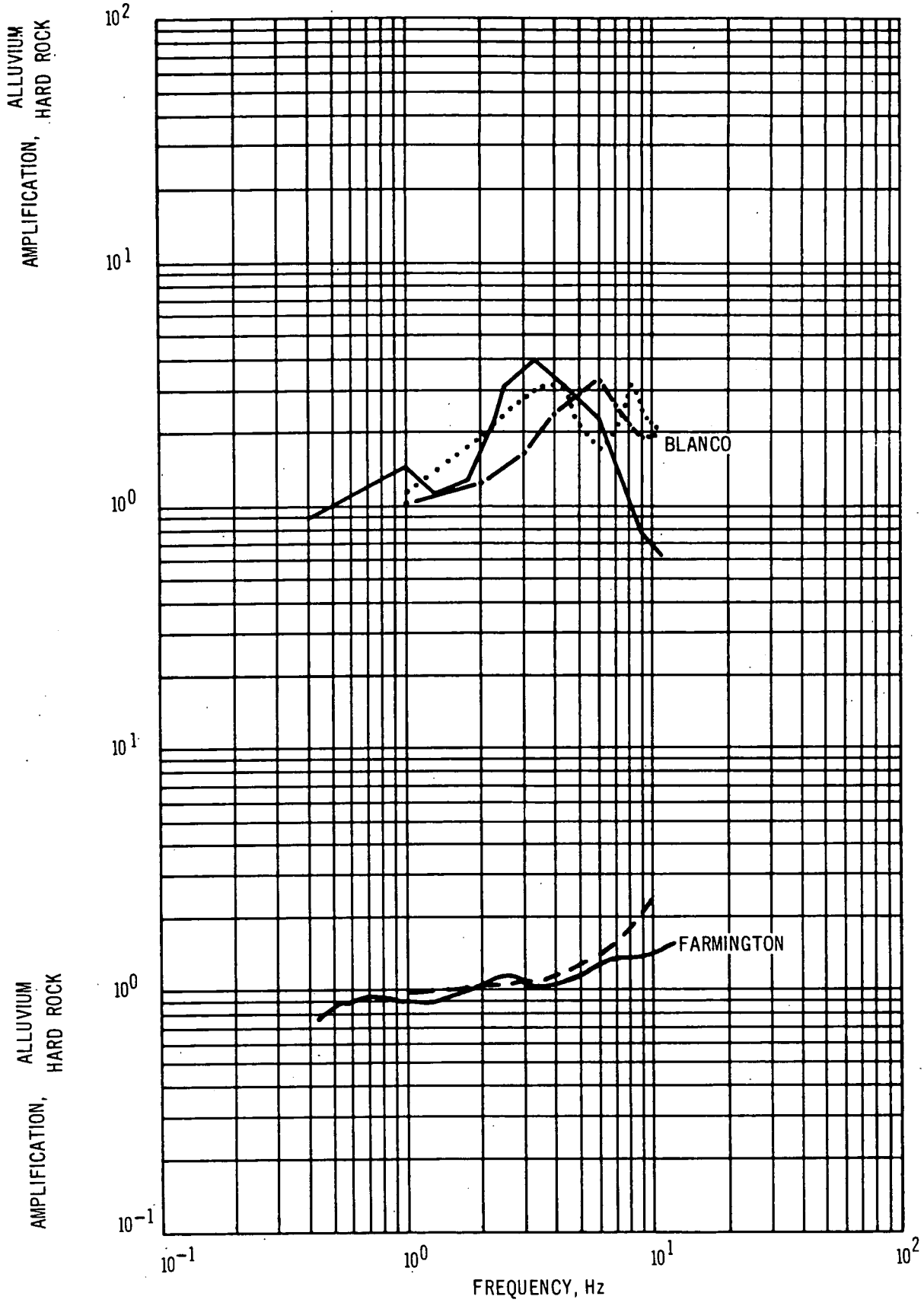

Figure B-13. Comparison of Observed (solid line) and Calculated (dash and dotted lines) Amplification at Stations Blanco and Farmington

REFERENCES

B-1 Schultz, A.; "Magnification of Love Waves;" NVO-1163-80; Environmental Research Corporation; 1967.

B-2 Davis, A. H., and Murphy, J. R.; "Amplification of Seismic Body Waves by Low Velocity Surface Layers;" NVO-1163-130; Environmental Research Corporation; 1968.

B-3 Murphy, J R. and Davis, A. H.; "Amplification of Rayleigh Waves in a Surface Layer of Variable Thickness;" NVO-1163-175; Environmental Research Corporation; 1969.

B-4 Haskell, N.A.; Dispersion of Surface Waves on Multilayered Media; Bulletin of Seismological Society of America, Vol. 43; 1953.

B-5. Dobrin, M.B.,; *"Introduction to Geophysical Prospecting:"* McGraw Hill Book Company, Inc.; New York; 1952.

This page intentionally left blank

DISTRIBUTION–NVO-1163-180

Mr. R. A. Johnson, AEC/NVOO, Las Vegas, Nevada (2 copies)
Dr. R. L. Aamodt, LASL, Los Alamos, New Mexico (1 copy)
Dr. G. H. Higgins, LRL, Livermore, California (1 copy)
Dr. H. L. Reynolds, LRL, Livermore, California (1 copy)
Dr. G. C. Werth, LRL, Livermore, California (1 copy)
Dr. M. B. Biles, AEC/DOS, Hq., Washington, D.C. (1 copy)
Mr. J. S. Kelley, AEC/DPNE, Hq., Washington, D.C. (1 copy)
Maj. Gen. E. B. Giller, AEC/DMA, Hq., Washington, D.C. (2 copies)
Mr. P. L. Russell, USBM, Denver, Colorado (1 copy)
Mr. Wendell Mickey, USC&GS, Rockville, Maryland (1 copy)
Dr. W. E. Ogle, LASL, Los Alamos, New Mexico (1 copy)
Mr. R. W. Newman, LASL, Los Alamos, New Mexico (1 copy)
Dr. M. L. Merritt, Org. 5412, Sandia Corp., Albuquerque, New Mexico (1 copy)
Dr. W. D. Weart, Org. 5412, Sandia Corp., Albuquerque, New Mexico (1 copy)
DTIE, Oak Ridge, Tennessee (1 copy)
Dr. J. R. Banister, Sandia Corp., Albuquerque, New Mexico (1 copy)
Dr. W. S. Twenhofel, USGS, Denver, Colorado (1 copy)
Dr. J. A. Blume, John A. Blume & Associates, San Francisco, California (2 copies)
Mr. Richard Hamburger, AEC/DPNE, Hq., Washington, D.C. (1 copy)
Mr. Eberhardt Rechtin, ARPA, Washington, D.C. (1 copy)
Mr. L. E. Rickey, H&N, Las Vegas, Nevada (1 copy)
Mr. K. W. King, USC&GS, Las Vegas, Nevada (2 copies)
Dr. L. B. Werner, Isotopes, Inc., Palo Alto, California (1 copy)
Mr. T. F. Thompson, San Francisco, California (1 copy)
Dr. N. M. Newmark, University of Illinois, Urbana, Illinois (1 copy)
Mr. S. D. Wilson, Shannon & Wilson, Inc., Seattle, Washington (1 copy)
Dr. D. U. Deere, University of Illinois, Urbana, Illinois (1 copy)
Dr. G. B. Maxey, University Station, Reno, Nevada (1 copy)
Mr. L. G. vonLossberg, Sheppard T. Powell & Associates, Baltimore, Maryland (1 copy)
Dr. Benjamin Grote, TCD-B, DASA, Sandia Base, Albuquerque, New Mexico (2 copies)
Mr. D. Springer, LRL, Livermore, California (1 copy)
Dr. Fred Holzer, LRL, Livermore, California (1 copy)
Dr. J. W. Hadley, LRL, Livermore, California (1 copy)
Mr. R. R. Loux, AEC/NVOO, Las Vegas, Nevada (1 copy)
Mr. Charles Atkinson, USBM, Bartlesville, Oklahoma (1 copy)
Resident Manager, H&N, Inc., Mercury, Nevada (1 copy)
Environmental Research Corporation, Las Vegas, Nevada (1 copy)
Environmental Research Corporation, Alexandria, Virginia (3 copies)